SYNTHESIS, CHARACTERISATION OF MIXED METAL OXIDE BASED INORGANIC MATERIALS AND IT'S APPLICATION TOWARDS THE REMOVAL OF FLUORIDE AND HEAVY METALS FROM CONTAMINATED WATER

Summary of Work (5000 Words)

Sarat Kanrar

Department of Chemistry

Presidency University

Registration No.: R-17RS205110096

Date of Registration: 10/07/2018

PRESIDENCY UNIVERSITY
KOLKATA

Supervisor

Dr. Sasikumar Palani

Department of Chemistry

Presidency University

Kolkata 700073, India

Table of Content

Title	Page No.
1. Introduction	3-7
1.1. Water Pollution: An existent and escalating matter of concern	
1.2. Nanomaterials as adsorbents for water treatment	
1.3. Remediation methods	
1.4. Research background	
1.5. Aim and objectives of the present work	
2. Materials and Methods	8-11
2.1. Chemical Reagents and Apparatus	
2.2. Synthesis of adsorbents	
2.3. Experimental procedures	
3. Results and Discussion	12-13
3.1. Adsorbent characterization of CZ	
3.2. Adsorbent characterization of CZL	
3.3. Adsorbent characterization of CB@CZ	
4. Batch Adsorption Study	13-15
4.1. Equilibrium analysis	
4.1.1. Adsorption isotherm model study for CZ	
4.1.2. Adsorption isotherm study for both removal of F- and Cu(II) by CZL	
4.1.3. Adsorption isotherm study for CB@CZ	
5. Summary	16
6. Acknowledgement	16
7. References	17-21
8. Table file	22-25
9. Figure file	26-33
10. Lists of Publications	34
11. National & International Seminar, Conference & Presentation	35

Introduction

1.1. Water Pollution: An existent and escalating matter of concern

Water is often a necessary component of life and a fundamental component of the ecosystem. The contamination of urban and industrial water by numerous contaminants and their toxicity puts the entire globe in significant concern. They're known to be extremely hazardous, non-biodegradable, and carcinogenic even at low quantities. Here is a table chart showing contaminants, their maximum permitted limits, and their hazardous consequences.

Containments	**Maximum permissible limits ($Mg\ L^{-1}$) WHO standard**	**Toxic effects**	**Reference**
Fluoride [F^-]	1.5	Dental and skeletal fluorosis, impaired thyroid function, cognitive delays, decrease in birth rate, muscle fiber degeneration etc.	[1]
Nitrate [NO_3^-]	50	Blue child syndrome babies, increased heart rate, nausea, headaches, abdominal cramps and increased risk of cancer, especially gastric cancer.	[2]
Chromium [Cr(VI)]	0.05	Diarrhea, stomach and intestinal bleedings, cramps, and liver and kidneydamage.	[3]
Copper [Cu(II)]	2.0	Nausea, vomiting, diarrhea, hematuria, jaundice, Wilson's, Parkinson's,Alzheimer's and other prion illnesses.	[4]
Nickel [Ni(II)]	0.05	Cardiac arrest, pneumonia, brain hemorrhage, liver damage, heart damage,carcinogenic and death.	[5]
Cadmium [Cd(II)]	0.003	Nausea, vomiting, diarrhea, muscle cramps, salivation, sensory disturbances, liver injury, convulsions,	[6]

		shock and renal failure	
Lead [Pb(II)]	0.05	Plumbism, nervous disorder, memory loss, convulsions, nausea, cerebraldisorder, diarrhea, circulatory disorder and could also be fatal at times.	[7]
Arsenic [AS(V)]	0.01	Cancer, thickening and discoloration of the skin, problems with bloodvessels, high blood pressure, and heart disease	[8]
Mercury [Hg(II)]	0.001	Damage to the central nervous system, impairment of pulmonary andkidney function, chest pain and dyspnea.	[9]
Zinc [Zn(II)]	5.0	Muscular stiffness, irritability, gastrointestinal distress, growth retardation, lung disorders, and even cancer	[10]
Iron [Fe (III)]	0.1	Nausea, vomiting, diarrhea and stomach pain.	[11]

1.2. Nanomaterials as adsorbents for water treatment

Various nanomaterials have been developed and employed for the elimination of aquatic contaminants in recent years. Nanomaterials are defined as any purposely generated particle with a characteristic dimension ranging from 1 to 100 nm, and they can take on a variety of intriguing morphologies, including spheres, tubes, rods, prisms, thin films, and buds. They are better adsorbing materials than conventional materials for pollution prevention, treatment, and clean-up of long-term problems like hazardous waste sites because of their high porosity, small size, active surface, self-assembly potential, high specificity, high reactivity, and catalytic potential. The nanomaterials of d-block metal ions such as Ti(IV), Cr(III), Mn(II/IV), Fe(II/III), Co(II/III), Ni(II)], Cu(II) and Zn(II) of the 4th period, Zr(IV) of the 5th period, and earth metals like Ce(IV), La(III), and Sm(III) of the periodic table were utilized in their oxide/ hydroxide form and are emerging as new alternatives for the treatment of contaminants from water.

1.3. Remediation methods

Numerous technologies have been developed during the last few decades to eliminate excessive contaminates from the water. Ion exchange, membrane filtration, electrolysis, and adsorption are only a few examples. Adsorption has been identified as one of the finest available ways among them. **Table-2 lists a number of different removal strategies, along with their benefits and drawbacks.**

Methods	Advantages	Disadvantages	Reference
Precipitation—Coagulation	(i) Most used method, particularly at the community level. (ii) Simple Operation	(i) Low treatment efficiency. (ii) Requirement of skilled manpower.	[12]
Membrane Based Processes	(i) Highly effective technique. (ii) Works under a wide pH range.	(i) Relatively higher cost. (ii) May not be suitable for water with high salinity and TDS.	[13]
Ion-Exchange Method	(i) High removal efficiency. (ii) Retains the taste and color of water intact.	(i) High cost due to synthetic resin. (ii) Treated water sometimes has a low pH and high levels of chloride	[14]
Adsorption	(i) High efficiency (ii) Ease in operation. (iii) Cost effective.	(i) Process is dependent on pH. (ii) Regeneration is required	[15]

1.4. Research background

Fluoride is a common anionic contaminant found in ground water that comes from a variety of sources, including the slow dissolution of fluorine-containing rocks, various minerals, and geochemical deposits, as well as effluents from industries such as glass and ceramic production, semiconductor manufacturing, and so on. Copper, on the other hand, is one of the most harmful and dangerous heavy metal contaminants found in natural water as a result of numerous sectors such as electroplating, mining, batteries, textiles, and automotive. For the sake of human health and the environment, it is critical to develop a cost-effective technique and adsorbent for removing fluoride and copper ions from contaminated ground water and industrial effluent. Some traditional adsorbents, such as metal oxides, graphene-based materials, polymer/biopolymer composites, granular activated carbon, zeolite, layered double hydroxides, and agricultural/industrial waste, have been reported to remove fluoride and copper ions from aqueous medium. Various rare metals, such as Zr (IV), La(III), Ce(IV), and others, have sparked a lot of attention in recent years due to their high selectivity and affinity for fluoride and copper. Tables 3 and 4 provide the lists of adsorbents for fluoride and Cu(II) in order of their adsorption capacity.

Table 3: Comparison of adsorption capacity of fluoride ions on various adsorbents at different pH

Adsorbents	pH	q_e (mg g^{-1})	References
CeO_2/Mg–Fe layered double hydroxides	6-7	38.7–60.4	[16]
Fe-Mg-La triple-metal composite	4	270.3	[17]
Fe-Al-La trimetal hydroxides	6.8 ± 0.2	74.07	[18]
Al(III)–Zr(IV) binary oxide	2	114.54	[19]
Fe–Al–Ce trimetal oxide	6.0–6.5	178	[20]
Mg-Al-Ce triple-metal composites	3.0–3.5	124.9	[21]
Manganese-magnesium-aluminum ternary metal oxide	7	63.05	[22]
Y-Zr-Al tri-metal nanocomposite	7	31	[23]
Mg/Fe layered double hydroxides	5	50.91	[24]
Hydrous CeO_2-Fe_3O_4 decorated polyaniline	6	116.28	[25]
Mg-Mn-Zr impregnated activated carbon	7	26.67	[26]
Lanthanum loaded chitosan−β-cyclodextrin composite	7	8.14	[27]
rGO/ZrO_2	7	46	[28]

Table 4: Comparison of adsorption capacity of Cu(II) ions on various adsorbents at different pH

Adsorbents	pH	q_e	References

		(mg g^{-1})	
Fe_2O_3@Microalgae composite	5.3 ± 0.1	38.68	[29]
TA@CNF-CDA aerogels	5	45.6	[30]
CD-HNT400	9.25	25.6	[31]
Nano structured titanium(IV) oxide	5	47.17	[32]
CMC-Alg/GO 5%,	5	64	[33]
CDAA	3.6	107.37	[34]
PAN-P-Ag	5	52.3	[35]
GO/cellulose	4.5	26.6	[36]
GO-HBP-NH_2-CMC	5	137.48	[37]
graphene oxide/MWCNTs /Fe_3O_4	7	20.83	[38]
HA-nHAP	5	35.24	[39]
M-CTS	4	192.31	[40]

1.5. Aim and objectives of the present work

The current research focuses on producing cost-effective, non-toxic, innovative mixed metal oxide based inorganic materials as adsorbents with high scavenging capacity for fluoride and heavy metal ion removal from contaminated water. The study is pursuing primary objectives in order to achieve this goal.

(i) To develop, synthesis, and characterize the binary [Cr(III)-Zr(IV)] named CZ or ternary mixed metal oxide [Ce(IV)- Zr(IV)-La(III)] based inorganic sorbent (including purity, crystallinity, surface morphology, particle size, surface area, thermal stability, surface charge densities at different pH and isoelectric point).

(ii) Surface modification of CZ with Chitosan and β–Cyclodextrin was carried out with the intention of expanding the use for Cu(II) removal.

(iii) To investigate the adsorption behavior of the adsorbent towards fluoride and heavy metal ions from a model contaminated water sample (with an emphasis on initial concentration, temperature, adsorbent dose, pH, contact time, stirring speed, kinetics, isotherm, thermodynamics, foreign ions effect, and regeneration) (made in a lab at a specific concentration)

(iv) Extend the study towards the potential applicability of the prepared adsorbent to removal of fluoride and heavy metal ions from a variety of contaminated water sources.

2. Materials and Methods

2.1. Chemical Reagents and Apparatus

Table 5 lists the number of chemicals employed in the synthesis of adsorbents and the preparation of various stock solutions. All of the compounds used in this study were analytical grade and were used without further purification. Double deionized water was used throughout the trials. Before the use of the all glassware were washed with dilute HNO_3 solution and then followed by thoroughly with double distilled water and acetone to remove any contaminant.

Table 5. List of the chemicals along with their formulas and company names

Name of Chemicals	Chemical formula	Company name
Zirconium(IV) oxide chloride octa-hydrate	$ZrOCl_2.8H_2O$	Sigma Aldrich
Ammonium cerium(IV) nitrate	$(NH_4)_2Ce(NO_3)_6$	Merck
Lanthanum(III) chloride hepta-hydrate	$LaCl_3.7H_2O$	Sigma Aldrich
Chromium(III) chloride hexahydrate	$CrCl_3.6H_2O$	Merck
Iron(III) chloride hexahydrate	$FeCl_3.6H_2O$	Merck
Aluminum chloride	$AlCl_3.6H_2O$	Merck

hexahydrate		
Sodium fluoride	NaF >99.9%	Sigma Aldrich
Copper sulphate pentahydrate	$CuSO_4.5H_2O$	Merck
Potassium dichromate	$K_2Cr_2O_7$	Merck
Nickel chloride hexahydrate	$NiCl_2.6H_2O$	Merck
Sodium nitrate	$NaNO_3$	Merck
Potassium permanganate	$KMnO_4$	Merck
Hydrogen peroxide	H_2O_2 30 wt%	Merck
Sodium hydroxide	NaOH	Merck
Hydrochloric acid	HCl, >98.0%	Merck
Nitric acid	HNO_3 70%	Merck
Liquor ammonia	NH_3, >99.98%	Merck
Sodium sulfate	Na_2SO_4	Merck
Sodium bicarbonate	$NaHCO_3$	Merck
Sodium phosphate monobasic	NaH_2PO_4	Merck
Calcium(II) chloride hexahydrate	$CaCl_2.6H_2O$	Merck
Magnesium(II) chloride hexahydrate	$MgCl_2.6H_2O$	Merck
Graphite flakes		Alfa Aesar
Ethanol	CH_3CH_2OH	Merck

2.2. Synthesis of adsorbents

2.2.1. Preparation of Cr(III)-incorporated Zr(IV) bimetallic oxide (CZ)

The Cr(III)-incorporated Zr(IV) oxide (CZ) was prepared using a co-precipitation procedure. In short, for the CZ material, a Cr:Zr ratio of (1:3,mol/mol) was used, and the schematic synthesis process of CZ is shown below.

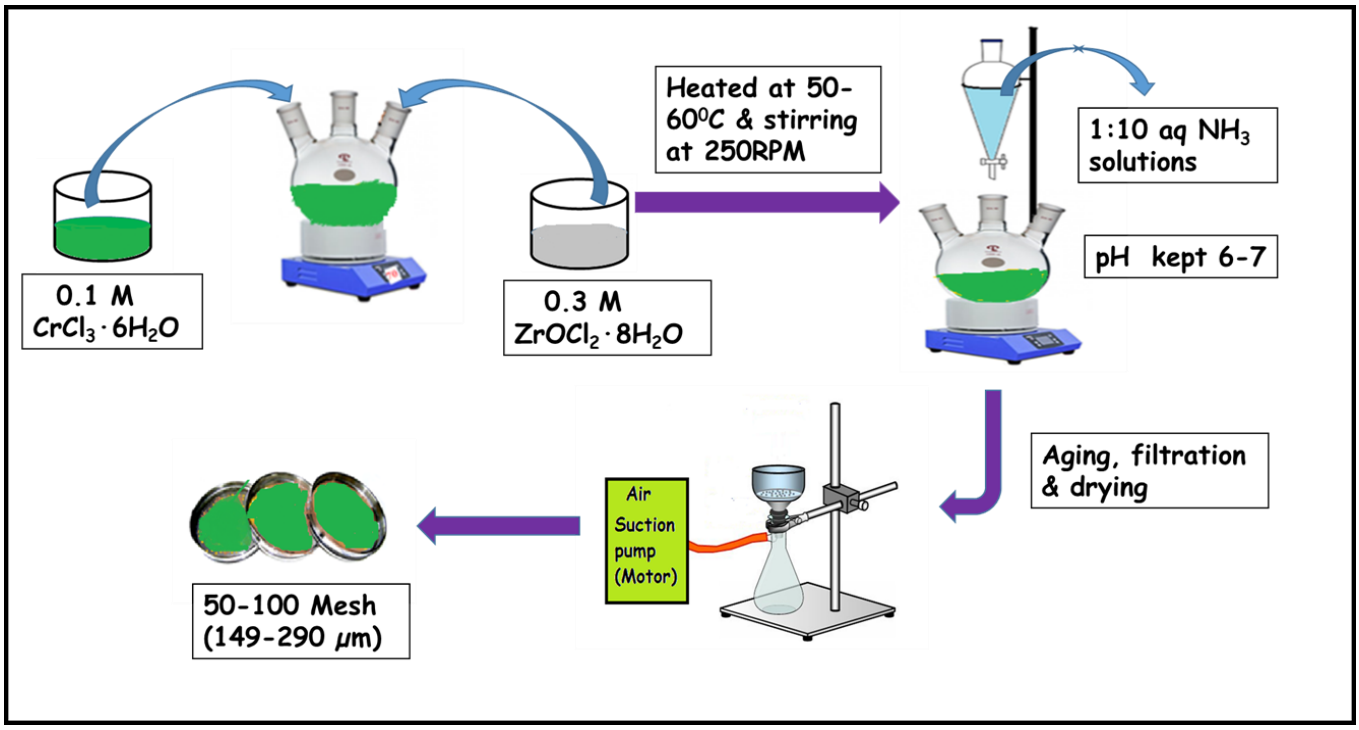

2.2.2. Preparation of Ce-Zr-La trimettalic oxide (CZL)

The schematic representation of synthesis of Ce-Zr-La trimettalic oxide (CZL) is given below-

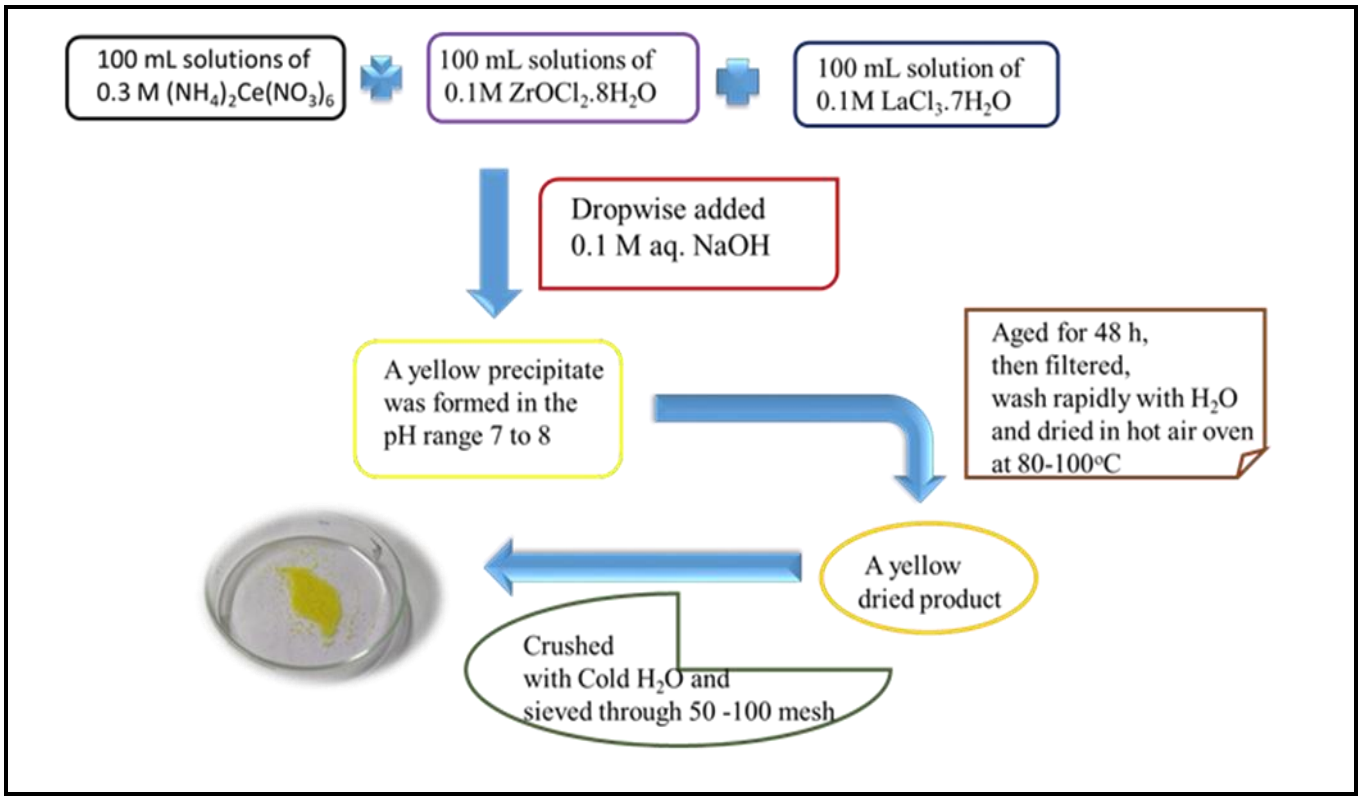
100 mL solutions of 0.3 M $(NH_4)_2Ce(NO_3)_6$
100 mL solutions of 0.1M $ZrOCl_2.8H_2O$
100 mL solution of 0.1M $LaCl_3.7H_2O$
Dropwise added 0.1 M aq. NaOH
A yellow precipitate was formed in the pH range 7 to 8
Aged for 48 h, then filtered, wash rapidly with H_2O and dried in hot air oven at 80-100°C
A yellow dried product
Crushed with Cold H_2O and sieved through 50 -100 mesh

2.2.3. Synthesis of Cr(III)/ Zr(IV) modified with chitosan grafted onto β-cyclodextrin (CB@CZ)

The following procedure was used for preparation of chromium/zirconium embedded with chitosan grafted onto β-cyclodextrin (CB@CZ). 1 g of chitosan powder in 100 mL of 2 % (v/v) in acetic acid solution, and 1g of β-cyclodextrin (β-CD) powder in 100 mL aqueous solution at 50-60°C were prepared separately. In a separate beaker, 100 mL solution of $CrCl_3 \bullet 6H_2O$ and $ZrOCl_2 \bullet 8H_2O$ admixture with a preselected molar ratio of 1:3 was prepared in 0.1M HCl. All the three solutions were mixed slowly and the final mixtures were stirred vigorously for 1 h, at ambient condition. After that, solutions of 1M NaOH were added drop wise to the mixture with constant stirring to bring the final pH of the solution to 8. The solution left to age for 24 h. The dark green coloured composite deposited was filtered and rinsed multiple times with double deionized water to remove any unreacted metal ions. The final dark green material dried in a hot air oven at 110 °C for 24 h. The bulk materials obtained were crushed into agglomerated particles with sizes ranging from 140–290 mm (52–100 mesh) before being used in all tests. For comparison B@CZ and C@CZ composite were also prepared using the same procedure but without the addition of chitosan and β-cyclodextrin (β–CD) respectively.

3.1. Experimental procedures

The batch adsorption approach was used to investigate the adsorption of Cu(II) ions. Batch experiments were conducted to analyse the effects of various parameters such as adsorbent dose, adsorption kinetics, and adsorption isotherm, as well as to determine the values of adsorbent adsorption capacities. All adsorption studies were carried out in a well-capped 250-ml polyethylene bottle with a specific amount of adsorbent and 50 ml of a specific adsorbate solution of precisely determined initial concentration (C_0, mg L^{-1}). After keeping the pH of the solution constant using 0.1 M HCl or 0.1 M NaOH, the experiment was carried out in a thermostat shaker and agitated at 250 (±5) rpm while maintaining the reaction temperature and agitation time. The solid from each reaction mixture was separated using a 0.45 mm Whatman® membrane filter immediately after the agitation period ended, and the residual concentration of the solution in the filtrate was determined. The mass balance formula (Eq.1) was used to compute the adsorbent's adsorption capacity (q_e, mg g^{-1}) as shown in Table 6.

3. Results and Discussion

3.1. Adsorbent characterization of CZ

Based on the results of primary experimental data as obtained from the mole variation of Cr(III) and Zr(IV), it was seen that the optimized CZ-material is with molar ratio 1:3 (Cr:Zr) which had been characterized elaborately. Surface morphologies and elemental distribution map of as-prepared CZ material was well characterized and presented in figure 1 (a to h). FESEM images of CZ exhibit the regular but rough surface morphology indicating that the material is very robust. The EDX spectrum of CZ confirms the presence of Cr, Zr Fig. 1 (g). The atomic percentage figure 1 (h) of Cr(III) and Zr(IV) in CZ obtained as 9.29 and 25.60% respectively, which has satisfied the desired composition of 1:3 (Cr:Zr) in CZ. The approximate chemical formula of the adsorbent is $ZrCr_{2.76}O_7$. The HRTEM image of CZ are presented in figure 1 (b) and indicates the uniform distribution of all elements without any agglomeration. Powder XRD pattern of CZ Fig. 1 (i) has shown absence of any sharp peak between diffraction angles of 10-90° conforms the amorphous nature of CZ. This nature of the material is indicating the higher surface area of the material than the crystalline one. A broad peak obtained at (2θ) 30.1◦, 32.7◦ and 58.2◦ which is due to the presence of ZrO_2 and Cr_2O_3 in the (JCPD file no 12-559) adsorbent.

3.2. Adsorbent characterization of CZL

Based on the results of primary experimental data as obtained from the mole variation of Ce(III), La(III) and Zr(IV), it was seen that the optimized CZL-material is with molar ratio 3:1:1 (Ce: Zr:La) which had been characterized elaborately. The surface morphology on the CZL composite was illustrated in Fig. 2a to h. It can be seen that, the FESEM images of CZL samples have amorphous structure and composed of the irregular size and flaky shape. The elements content of CZL in the samples were shown in Fig. 2 (g to h) and it is clear that La, Zr, Ce and O appeared in the EDS spectrum. The atomic percentage figure 2 (h) of Ce(III), La(III) and Zr(IV) in CZL obtained as 11.05, 1.51 and 4.47% respectively, which has satisfied the desired composition of 3:1:1 (Ce:Zr:La) in CZL. Furthermore, SEM-EDS can provide a powerful tool in mapping mode to analysed the elemental distribution and to determine the compositions of the elements on the surface of adsorbents. The XRD patterns of the CZL were shown in Fig. 2 (i) and it can be seen that the samples had sharp and robust diffraction peaks. The diffraction peaks at 28.53° and 47.48°are attributed to CeO_2 (JCPDS 02- 1306).

The FT-IR spectra of CZL adsorbent were shown in Fig. 2 (j) and the typical peaks of functional groups can be discovered. The bands at 3437 cm^{-1} are ascribed to the hydroxyl groups (O–H) stretching vibration and the one at 1636 cm^{-1} corresponds to the hydroxyl groups (O–H) bending vibrations.

3.3. Adsorbent characterization of CB@CZ

The FESEM images of the synthesized CB@CZ composite were shown in Fig. 3a. From a visual observation, composite showed a nonporous and smooth fluffy surface. EDX analysis of CB@CZ verifies the presence of three intense peaks of C along with N and O which represent the major elements of the adsorbent (Fig. 3 g to h). Furthermore, elemental mapping was employed in order to have better insights on the chemical composition and the spatial distribution of elements on the surface of CB@CZ and the results were displayed in Fig. 3 (b) to f. XRD pattern of CB@CZ nanocomposite was illustrated in Fig. 3 (i) and shown absence of any sharp peak between diffraction angles of 10-90° conforms the amorphous nature of CB@CZ. Fig. 3 (j) presents a FT–IR spectrum of CB@CZ ad showed a broad peak at 3430 cm^{-1} which is assigned to the stretching vibration of O–H and N–H. Symmetric and asymmetric C–H groups are observed at 2932 cm^{-1}. Absorption band at 1638 cm^{-1} (C–O stretching) corresponding to chitin moiety in chitosan. The peaks at 1386 cm^{-1} and 1149 cm^{-1} represent C–H bending and C-O-C stretching, respectively.

4. Batch Adsorption Study

4.1. Equilibrium analysis

4.1.1. Adsorption isotherm model study for CZ

To understand the mechanistic pathway of fluoride adsorption reaction on CZ surface and to obtain the maximum adsorption capacity of the newly prepared CZ, the adsorption isotherm studies are basic requirement. The adsorption isotherm experiments were performed at four different temperatures (283, 293, 303, and 313 K) and neutral pH (7 ± 0.2) taking initial concentration of fluoride solution ranged in 10 to 300 mg L^{-1} as shown in fig. 4. The observed adsorption dataset of fluoride removal experiments were modelled with four basic isotherm models such as Langmuir (Eq. iv), Freundlich (Eq. v), Redlich- Peterson (RP) (Eq. vi), and Dubinin-Radushkevich (D-R) (Eq. vii) as presented in Table 6. From the equilibrium study, the maximum adsorption capacity obtained 90.67 mg g^{-1}. From Table 7, it is observed that the correlation coefficients (R^2) of Freundlich isotherm were closest to 1.

Therefore, it infers the adsorption of fluoride over adsorbent is heterogeneous surface coverage with multilayer adsorption. The g value obtained from Redlich-Peterson model is less than 1; this also supports the heterogeneous surface coverage with multilayer adsorption phenomena. D-R isotherm model also well adheres with experimental data. Analogous observation also reported by other researchers. The trend of adherences of data fitting is follows as DR ≈ Freundlich > Redlich Peterson > Langmuir. Mean free energy of the adsorption (EDR) is an important parameter to determine the nature of the adsorption mechanism and is defined as the amount of free energy change involved to transfer 1 mol of adsorbate from infinity to the adsorbent surface. The calculated EDR value at different temperatures are between 9.8 and 11.4 kJ mol^{-1} (Table 12) indicating the ion-exchange nature of the reaction.

4.1.2. Adsorption isotherm study for both removal of F^- and Cu(II) by CZL

The isotherm studies were performed for removal of fluoride with two different pH 5.01 and 7.02 and the nonlinear fitting curve were shown in fig 5 (a) and (b) respectively and the correlation coefficients (R^2) values for Langmuir, Freundlich, and R-P isotherms were compared and others associated parameters were presented in Table 8. From the table, it was observed that the Freundlich (R^2> 0.97, 0.98), isotherms model was more suitable with the experimental data of fluoride with both pH of solutions, indicated the appearance of heterogeneous adsorption and n > 1 also suggests that the adsorption process was favourable. The experimental data of fluoride was also obeyed with the Redlich–Peterson isotherm model and the value of g was 0.55 and 0.57 at pH 5.01 and 7.02 respectively; suggested that the greater conformity of the experimental data with the Freundlich isotherm. The maximum adsorption capacity for fluoride calculated by Langmuir isotherm model and results showed that q_m (mg g^{-1}) values for fluoride were 213.99 and 157.07 mg g^{-1} at pH 5.01 and 7.02 respectively at 303K. Moreover, for better analysis experiments were performed at four different temperatures and at pH 7.02 as depicted in fig 5 (c) and (d) and resultant parameters were shown in Table 9. As expected Freundlich isotherm was best fitted model for fluoride at four different temperatures and values of n and K_F increased with increasing temperatures, suggested that an increase in the adsorption intensity with increasing T on the reactions and the adsorption processes were endothermic in nature. Similarly, for Cu(II) adsorption process, the non-linear fitting plots of three different isotherm models at four different temperatures from 283 to 313K were presented in Fig. 6 (a) to (d), respectively and the calculated isotherm parameters along with correlation coefficients were shown in Table 10. By evaluating the R^2 values, it was predicted that the Langmuir isotherm

model gave a more satisfactory fitting result with experimental data. The closeness of the "g" value (R−P isotherm parameter) to 1 at different temperatures, suggested with the good fit of Langmuir isotherm. The maximum Cu(II) adsorption capacity of CZL was 61.52 mg g^{-1} at 313K and adsorption process was mainly homogeneous and monolayer adsorption. The dimensionless separation factor [$R_L = (1 + K_L C_e)^{-1}$] was used to determine the favourability of the adsorption process for Cu(II). R_L values were found less than 1 suggested that Cu(II) adsorption on CZL was a favourable process.

4.1.3. Adsorption isotherm study for CB@CZ

A non-linear fit of Langmuir and Freundlich adsorption isotherms at four different temperatures were shown in Fig. 7 and the relevant parameters were listed in Table 10. As presented, the values of the regression co-efficient R^2 of Langmuir isotherm model were higher than Freundlich isotherm at four different temperatures, which indicated Langmuir isotherm model showed better description to simulate the isothermal adsorption process and that's mean a monolayer of Cu(II) was probably adsorbed onto the CB@CZ surfaces at equilibrium. The maximum adsorption capacity for Cu(II) calculated by Langmuir isotherm model and results showed that qm (mg g^{-1}) values for Cu(II) was 63.84 at pH 5.01 at 313K. The large numbers of hydroxyl, amino and carboxyl groups on the CB@CZ nanocomposite will provide large numbers of adsorption sites and that's why the adsorbent had a much higher affinity and adsorption capacity for Cu(II). The R_L values were found less than 1 and n values from Freundlich model were greater than 1 at all four different temperatures, suggested that Cu(II) adsorption onto CB@CZ was a favourable process. Moreover values of K_L and qm were increases with temperatures, indicating increase of thermally accessible with strong affinity between Cu(II) and CB@CZ.

5. Summary

- The cost-effective efficient pristine nanocomposite consists Cr(III)-incorporated Zr(IV) oxide (CZ) was synthesized in a very simple chemical route for removal of fluoride from contaminated water and characterized extensively by various sophisticated techniques. The maximum adsorption capacity obtained 90.67 mg g^{-1}. The observed results show that the adsorbent material CZ is suitable for the lab as well as field application.

- A new composite CB@CZ was prepared by surface modification of CZ with Chitosan and β-cyclodextrin and successfully applied for removal of Cu(II). The solution pH greatly affects the adsorption of Cu(II) onto CB@CZ and the kinetics of Cu(II) adsorption follows the pseudo-second-order model. The equilibrium data are fitted well by the Langmuir model of adsorption. Results of this work suggest that the CB@CZ may be promising adsorbents for the removal of heavy metal ions from wastewater.

- A novel Ce-Zr-La trimetal composite (CZL) was successfully developed by a one-step co-precipitation approach and used for both the adsorption of fluoride as well as Cu(II) from aqueous solutions. The maximum adsorption capacities of 213.99 and 157.07 mg g^{-1} were achieved at pH 5.01 and 7.02 respectively for fluoride ions and 61.52 mg g^{-1} at 313K for Cu(II) ions. Thus, CZL should have good prospect in the light of decontamination of F^- and Cu(II) from the contaminated ground waters.

6. Acknowledgement

To begin, I'd want to convey my heartfelt gratitude and respects to my supervisor, Dr. Sasikumar Palani, for his steadfast assistance, essential guidance, and continuous encouragement during my research. I'd want to express my gratitude to Dr. Uday Chand Ghosh (Ex-Associate Professor, Department of Chemistry, Presidency University) for his advice, love, and unwavering support and cooperation in helping me finish my project. I would like to show my thankfulness to the University Grants Commission (UGC), Government of India, for providing me with a fellowship and financial aid. I am grateful to the Department of Chemistry at Presidency University in Kolkata, India, including the Authority, for providing the laboratory space for this research.

7. References

1) Sneha Jagtap, Mahesh Kumar Yenkie, Nitin Labhsetwar, and Sadhana Rayalu, Fluoride in Drinking Water and Defluoridation of Water. Chem. Rev. 112 (2012) 2454–2466. **https://dx.doi.org/10.1021/cr2002855.**

2) Narada Bombuwala Dewage, Achala S. Liyanage, Charles U. Pittman Jr, Dinesh Mohan, Todd Mlsna, Fast nitrate and fluoride adsorption and magnetic separation from water on α-Fe2O3 and Fe3O4 dispersed on Douglas fir biochar. Bioresource Technology 263 (2018) 258–265. **https://doi.org/10.1016/j.biortech.2018.05.001.**

3) Yi Lu, Bin Jiang, Liang Fang, Faling Ling, Jiemei Gao, Fang Wu, Xihua Zhang, High performance NiFe layered double hydroxide for methyl orange dye and Cr(VI) adsorption. Chemosphere 152 (2016) 415-422. **http://dx.doi.org/10.1016/j.chemosphere.2016.03.015.**

4) Xubing Sun, Jiayong Zhang, Yaohui You, Enhancement of Cu(II) removal by carbon disulfide modified black wattle tannin gel. Colloids and Surfaces A 608 (2021) 125594. **https://doi.org/10.1016/j.colsurfa.2020.125594.**

5) Anderson B. Pires, Luciano Vitali, Amanda Tavares, Carlos A. Germano, Su´elen M. Amorim, Regina F.P.M. Moreira, Rosely A. Peralta, Ademir Neves, Chitosan functionalized with heptadentate dinucleating ligand applied to removal of nickel, copper and zinc. Carbohydrate Polymers 256 (2021) 117589. **https://doi.org/10.1016/j.carbpol.2020.117589**.

6) Junyong He, Yulian Li, Chengming Wang, Kaisheng Zhang, Dongyue Lin, Lingtao Kong, Jinhuai Liu, Rapid adsorption of Pb, Cu and Cd from aqueous solutions by β-cyclodextrin polymers. Applied Surface Science 426 (2017) 29-39. **http://dx.doi.org/doi:10.1016/j.apsusc.2017.07.103.**

7) 7. Xinyi Xu, Xiao-kun Ouyang, Li-Ye Yang, Adsorption of Pb(II) from aqueous solutions using crosslinked carboxylated chitosan/carboxylated nanocellulose hydrogel beads. Journal of Molecular Liquids. 322 (2021) 114523. **https://doi.org/10.1016/j.molliq.2020.114523.**

8) Sridhar Vadahanambi, Sang-Heon Lee, Won-Jong Kim and Il-Kwon Oh, Arsenic Removal from Contaminated Water Using Three-Dimensional Graphene-Carbon Nanotube-Iron Oxide Nanostructures. Environ. Sci. Technol. 47 (2013) 10510−10517. **https://dx.doi.org/10.1021/es401389g.**

9) Efstathios V. Liakos, Mariza Mone, Dimitra A. Lambropoulou, Dimitrios N. Bikiaris and George Z. Kyzas, Adsorption Evaluation for the Removal of Nickel, Mercury, and Barium Ions from

Single-Component and Mixtures of Aqueous Solutions by Using an Optimized Biobased Chitosan Derivative. Polymers 13 (2021) 232. **https://doi.org/10.3390/polym13020232.**

10) Sharafat Ali, Syed Aziz Ur Rehman, Izaz Ali Shah, Muhammad Usman Farid, Alicia Kyoungjin An, Haiou Huang, Efficient removal of zinc from water and wastewater effluents by hydroxylated and carboxylated carbon nanotube membranes: Behaviors and mechanisms of dynamic filtration. Journal of Hazardous Materials 365 (2019) 64–73. **https://doi.org/10.1016/j.jhazmat.2018.10.089.**

11) Khalfa. Leila, Cervera, M. Luisa, Souissi-najjar, Soaad and Bagane, Mohamed, Removal of Fe (III) from synthetic wastewater into raw and modified clay: Experiments and models fitting. Separation Science and Technology 56 (2021) 708-718. **http://dx.doi.org/10.1080/01496395.2017.1323923.**

12) Yidong Zou, Xiangxue Wang, Zhongshan Chen, Wen Yao, Yuejie Ai, Yunhai Liu, Tasawar Hayat, Ahmed Alsaedi, Njud S. Alharbi, XiangkeWang, Superior coagulation of graphene oxides on nanoscale layered double hydroxides and layered double oxides. Environmental Pollution 219 (2016) 107–117. **https://doi.org/10.1016/j.envpol.2016.10.052.**

13) Mekdimu Mezemir Damtie, Yun Chul Woo, Bongchul Kim, Ruth Habte Hailemariam, Kwang-Duck Park, Ho Kyong Shon, Chanhyuk Park, June-Seok Choi, Removal of fluoride in membrane-based water and wastewater treatment technologies: Performance review. Journal of Environmental Management 251 (2019) 109524. **https://doi.org/10.1016/j.jenvman.2019.109524.**

14) Martyna Grzegorzek, Katarzyna Majewska-Nowak, Arif Eftekhar Ahmed, Removal of fluoride from multicomponent water solutions with the use of monovalent selective ion-exchange membranes. Science of the Total Environment 722 (2020) 137681. **https://doi.org/10.1016/j.scitotenv.2020.137681.**

15) Chunsheng Lei, Xiaofeng Zhu, Bicheng Zhu, Chuanjia Jiang, Yao Le, Jiaguo Yua, Superb adsorption capacity of hierarchical calcined Ni/Mg/Al layered double hydroxides for Congo red and Cr (VI) ions. Journal of Hazardous Materials 321 (2017) 801–811. **http://dx.doi.org/10.1016/j.jhazmat.2016.09.070.**

16) Tao Zhang, Qiurong Li, Haiyan Xiao, Zhenyu Mei, Hongxiao Lu, Yuming Zhou, Enhanced fluoride removal from water by non-thermal plasma modified CeO_2/Mg–Fe layered double hydroxides. Applied Clay Science 72 (2013) 117–123. **http://dx.doi.org/10.1016/j.clay.2012.12.003.**

17) Yang Yu, Ling Yu, J. Paul Chen, Adsorption of fluoride by Fe-Mg-La triple-metal composite: adsorbent preparation, illustration of performance and study of mechanisms. Chemical Engineering Journal 262 (2015) 839–846. **http://dx.doi.org/10.1016/j.cej.2014.09.006.**

18) Li Li, Zhu Qi, Man Kexin, Xing Zipeng, Fluoride removal from liquid phase by Fe-Al-La trimetal hydroxides adsorbent prepared by iron and aluminum leaching from red mud. Journal of Molecular Liquids 237 (2017) 164–172. **http://dx.doi.org/10.1016/j.molliq.2017.04.097.**

19) Jiuya Zhu, Xiaoyan Lin, Pengwei Wu, Qiusheng Zhou, Xuegang Luo, Fluoride removal from aqueous solution by Al(III)– Zr(IV) binary oxide adsorbent. Applied Surface Science 357 (2015) 91–100. **http://dx.doi.org/10.1016/j.apsusc.2015.09.012.**

20) Xiaomei Wu, Yu Zhang, Xiaomin Dou, Min Yang, Fluoride removal performance of a novel Fe–Al–Ce trimetal oxide adsorbent. Chemosphere 69 (2007) 1758–1764. **http://dx.doi:10.1016/j.chemosphere.2007.05.075.**

21) Yaling Chi, Yuantao Chen, Chunlian Hu, YunshengWang, Chen Liu, Preparation of Mg-Al-Ce triple-metal composites for fluoride removal from aqueous solutions. Journal of Molecular Liquids 242 (2017) 416–422. **http://dx.doi.org/10.1016/j.molliq.2017.07.026.**

22) Ming Gao, Wei Wang, Mengbo Cao, Hongbing Yang, Yongsheng Li, Hierarchical hollow manganese-magnesium-aluminum ternary metal oxide for fluoride elimination. Environmental Research 188 (2020) 109735. **https://doi.org/10.1016/j.envres.2020.109735.**

23) Hualing Jiang, Xueqin Li, Lei Tian, Tao Wang, QiWang, Pingping Niu, Pinghua Chen, Xubiao Luo, Defluoridation investigation of Yttrium by laminated Y-Zr-Al tri-metal nanocomposite and analysis of the fluoride sorption mechanism. Science of the Total Environment 648 (2019) 1342–1353. **https://doi.org/10.1016/j.scitotenv.2018.08.258.**

24) Dongjuan Kang, Xiaolin Yu, Shengrui Tong, Maofa Ge, Junchao Zuo, Changyan Cao, Weiguo Song, Performance and mechanism of Mg/Fe layered double hydroxides for fluoride and arsenate removal from aqueous solution. Chemical Engineering Journal 228 (2013) 731–740. **http://dx.doi.org/10.1016/j.cej.2013.05.041.**

25) Marko Chigondo, Hugues Kamdem Paumo, Madhumita Bhaumik, Kriveshini Pillay, Arjun Maity, Hydrous CeO_2-Fe_3O_4 decorated polyaniline fibers nanocomposite for effective defluoridation of drinking water. Journal of Colloid and Interface Science 532 (2018) 500–516. **https://doi.org/10.1016/j.jcis.2018.07.134**.

26) Aditi Mullick, Sudarsan Neogi, Ultrasound assisted synthesis of Mg-Mn-Zr impregnated activated carbon for effective fluoride adsorption from water. Ultrasonics Sonochemistry 50 (2018) 126-137. . **https://doi.org/10.1016/j.ultsonch.2018.09.010.**

27) Jayaram Preethi and Sankaran Meenakshi, Fabrication of La^{3+} Impregnated Chitosan/ β-Cyclodextrin Biopolymeric Materials for Effective Utilization of Chromate and Fluoride Adsorption in Single Systems. Journal of Chemical & Engineering Data 63 (2018) 723−731. **https://doi.org/10.1021/acs.jced.7b00889.**

28) Sweta Mohan, Vijay Kumar, Devendra Kumar Singh and Syed Hadi Hasan, Synthesis and characterization of rGO/ZrO_2 nanocomposite for enhanced removal of fluoride from water: kinetics, isotherm, and thermodynamic modelling and its adsorption mechanism. RSC Adv. 90 (2016) 87523–87538. **https://doi.org/10.1039/c6ra15460c.**

29) Li Shen, Junjun Wang, Zhanfei Li, Ling Fan, Ran Chen, Xueling Wu, Jiaokun Li, Weimin Zeng, A high-efficiency Fe_2O_3@Microalgae composite for heavy metal removal from aqueous solution. Journal of Water Process Engineering 33 (2020) 101026. **https://doi.org/10.1016/j.jwpe.2019.101026.**

30) Yong Ji, Yingying Wen, Zhong Wang, Shifeng Zhang, Minjie Guo, Eco-friendly fabrication of a cost-effective cellulose nanofiber-based aerogel for multifunctional applications in Cu(II) and organic pollutants removal. Journal of Cleaner Production 255 (2020) 120276. **https://doi.org/10.1016/j.jclepro.2020.120276.**

31) Mohamed Triki, Haythem Tanazefti, Hafedh Kochkar, Design of β-cyclodextrin modified TiO_2 nanotubes for the adsorption of Cu (II): Isotherms and kinetics study. Journal of Colloid and Interface Science 493 (2017) 77–84. **http://dx.doi.org/10.1016/j.jcis.2017.01.028.**

32) Sushanta Debnath, Uday Chand Ghosh, Equilibrium modeling of single and binary adsorption of Cd (II) and Cu (II) onto agglomerated nano structured titanium (IV) oxide. Desalination 273 (2011) 330–342. **http://dx.doi.org/10.1016/j.desal.2011.01.043.**

33) Dalia Allouss, Younes Essamlali, Achraf Chakir, Samia Khadhar, Mohamed Zahouily, Effective removal of Cu(II) from aqueous solution over graphene oxide encapsulated carboxymethyl cellulose-alginate hydrogel microspheres: towards real wastewater treatment plants. Environmental Science and Pollution Research 27 (2020) 7476–7492. **https://doi.org/10.1007/s11356-019-06950-w.**

34) Zhanhua Huang, Shouxin Liu, Bin Zhang, Lili Xu, Xiaofeng Hu, Equilibrium and kinetics studies on the absorption of Cu(II) from the aqueous phase using a β-cyclodextrin-based

adsorbent. Carbohydrate Polymers 88 (2012) 609 – 617. **https://doi.org/10.1016/j.carbpol.2012.01.009.**

35) Qian Yang, Xiaoxin Guo, Xiufang Ye, Haijin Zhu, Lingxue Kong, Tingting Hou, Functionalized polyacrylonitrile fibers with durable antibacterial activity and superior Cu(II)-removal performance. Materials Chemistry and Physics 245 (2020) 122755. **https://doi.org/10.1016/j.matchemphys.2020.122755.**

36) Rafal Sitko, Marcin Musielak, Beata Zawisza, Ewa Talik, Anna Gagor, Graphene oxide/cellulose membranes in adsorption of divalent metal ions. RSC Adv. 6 (2016) 96595-96605. **https://doi.org/10.1039/C6RA21432K.**

37) Qiaoping Kong, Sergei Preis, Leli Li, Pei Luo, Yun Hu, Chaohai Wei, Graphene oxide-terminated hyperbranched amino polymer- Carboxymethyl cellulose ternary nanocomposite for efficient removal of heavy metals from aqueous solutions. International Journal of Biological Macromolecules 149 (2020) 581–592. **https://doi.org/10.1016/j.ijbiomac.2020.01.185.**

38) Zhihang Long, Yingqing Zhan, Fei Li, Xinyi Wan, Yi He, Chunyan Hou, Hai Hu, Hydrothermal synthesis of graphene oxide/multi walled carbon nanotube/Fe3O4 ternary nanocomposite for removal of Cu (II) and methylene blue. Journal of Nanoparticle Research 19 (2017) 1-16. **https://doi.org/10.1007/s11051-017-4014-4.**

39) Wei Wei, Xuan Han, Mengjia Zhang, Yong Zhang, Yong Zhang, Chunmiao Zheng, Macromolecular humic acid modified nano-hydroxyapatite for simultaneous removal of Cu(II) and methylene blue from aqueous solution: Experimental design and adsorption study. International Journal of Biological Macromolecules 150 (2020) 849–860. **https://doi.org/10.1016/j.ijbiomac.2020.02.137.**

40) Zetty Azalea Sutirman, Eka Amira Rahim, Mohd Marsin Sanagi, Khairil Juhanni Abd Karim, Wan Aini, Wan Ibrahim, New efficient chitosan derivative for Cu(II) ions removal: Characterization and adsorption performance. International Journal of Biological Macromolecules 153 (2020) 513–522. **https://doi.org/10.1016/j.ijbiomac.2020.03.015.**

Table File

Table 6: All model equations used to analyse the experimental results

Equation Name	Mathematical form	Equation No.
Mass- balance equation	$q_e = \frac{(C_0 - C_e) \times V}{m}$	(i)
Pseudo 1st order kinetic Model	$q_t = q_e\,(1 - e^{-k_1 t})$	(ii)
Pseudo 2nd order kinetic Model	$q_t = \frac{{q_e}^2\, k_2\, t}{(1 + q_e\, k_2\, t)}$	(iii)
Intra particle Diffusion kinetic Model	$q_t = K_{id} \times t^{\frac{1}{2}} + C$	(iv)
Langmuir Isotherm equation	$q_e = \frac{q_m K_L C_e}{1 + K_L C_e}$	(v)
Freundlich Isotherm equation	$q_e = K_f \times C_e^{\frac{1}{n}}$	(vi)
Redlich–Peterson equation	$q_e = \frac{\alpha C_e}{(1 + \beta C_e g)}$	(vii)
DR Isotherm equation	$q_e = q_s\, e^{(-\beta\varepsilon^2)}$	(viii)

Here, C_0 and C_e are the initial and equilibrium concentration of adsorbate solutions respectively (mg L^{-1}), m represent the weight of adsorbent (g) and V denotes the volume of experimental solution (L). q_e and q_t are the adsorption capacities (mg g^{-1}) at equilibrium and time, t (min), respectively, Ce (mg L^{-1}) is the concentration of the adsorbate at the equilibrium time, k_1 the pseudo- first order rate constant (min^{-1}). k_2 (g mg^{-1} min^{-1}) is the pseudo-second order rate constants, k_d (mg g^{-1} $min^{-0.5}$) denotes the intra-particle diffusion rate constant, C represents a constant associated to the periphery layer width (mg g^{-1})

q_m is the Langmuir monolayer capacity (mg g^{-1}), K_L is the energy of adsorption (L mg^{-1}) or Langmuir constant, and K_F, the Freundlich capacity (mg g^{-1}) and n is a dimensionless constant of Freundlich equation called adsorption intensity, α, β, and g are the Redlich-Peterson constant (unit less). From DR model equation, qs is the maximum adsorption capacity in mol kg^{-1}. β (mol^2 kJ^{-2}) is a constant of DR isotherm and ε^2 is related to the equilibrium adsorbate concentration, C_e (mol L^{-1}).

Isotherm	Parameter	283K	293K	303K	313K
Langmuir	q_m (mg g-1)	63.63	84.18	90.67	88.02
	K_L (L mg^{-1})	0.037	0.0189	0.0183	0.0261
	R^2	0.858	0.904	0.903	0.869
Freundlich	K_F ($mg^{1-1/n} L^n g^{-1}$)	12.92	9.47	10.05	13.29
	n	3.59	2.73	2.72	3.08
	R^2	0.933	0.917	0.935	0.946
Redlich–Peterson	α	25.66	32.43	42.90	40
	β	1.74	3.15	3.99	2.75
	g	0.743	0.647	0.643	0.691
	R^2	0.923	0.918	0.924	0.945
Dubinin–Radushkevich	q_s (mol kg^{-1})	1.56	1.86	1.89	1.86
	K_{ad} (mol^2 kJ^{-2}) $\times 10^3$	4.23	5.21	4.68	3.80
	E_{DR} (kJ mol^{-1})	10.88	9.80	10.34	11.48
	R^2	0.961	0.930	0.942	0.943

Table 8: Adsorption Isotherm Model Analysis for fluoride removal at 303K with two different pH by CZL

Isotherm	Parameter	pH=5.01	pH=7.02
Langmuir	**q_m (mg g^{-1})**	213.99	157.07
	K_L (L mg^{-1})	0.0079	0.0137
	R^2	0.963	0.948
Freundlich	**K_F ($mg^{1-1/n} L^n g^{-1}$)**	7.12	10.805
	n	1.819	2.232
	R^2	0.972	0.980
Redlich–Peterson	**α**	4.87	30.05
	β	0.340	2.431
	g	0.554	0.574
	R^2	0.968	0.978

Table 9: Adsorption Isotherm Model Analysis for fluoride removal at four different temperatures by CZL

Isotherm	Parameter	283K	293K	303K	313K
Langmuir	**q_m (mg g-1)**	128.71	151.50	157.07	158.76
	K_L (L mg^{-1})	0.012	0.013	0.0137	0.0139
	R^2	0.937	0.954	0.948	0.966
Freundlich	**K_F ($mg^{1-1/n} L^n g^{-1}$)**	8.48	9.74	10.80	10.64
	n	2.22	2.18	2.23	2.20
	R^2	0.940	0.955	0.935	0.967

Table 10: Adsorption Isotherm Model Analysis for Cu(II) removal at pH=5.01 with four different temperatures by CZL

Isotherm	Parameter	283K	293K	303K	313K
Langmuir	q_m (mg g-1)	49.51	55.23	55.85	61.52
	K_L (L mg^{-1})	0.043	0.039	0.038	0.028
	R^2	0.944	0.939	0.974	0.964
Freundlich	K_F ($mg^{1-1/n} L^n g^{-1}$)	6.80	9.47	6.65	5.33
	n	2.56	2.44	2.40	2.13
	R^2	0.941	0.864	0.948	0.958
Redlich–Peterson	α	3.388	2.299	2.406	2.483
	β	0.173	0.051	0.063	0.113
	g	0.814	0.955	0.922	0.795
	R^2	0.946	0.935	0.968	0.962

Table 11: Adsorption Isotherm Model Analysis for Cu(II) removal at pH=5.01 with four different temperatures by CB@CZ

Isotherm	Parameter	283K	293K	303K	313K
Langmuir	q_m (mg g-1)	52.82	60.06	70.04	76.47
	K_L (L mg^{-1})	0.025	0.022	0.021	0.019
	R^2	0.975	0.974	0.952	0.984
Freundlich	K_F ($mg^{1-1/n} L^n g^{-1}$)	4.52	5.03	5.79	4.57
	n	2.16	2.14	2.11	1.92
	R^2	0.980	0.991	0.988	0.971

Figure File

(A)

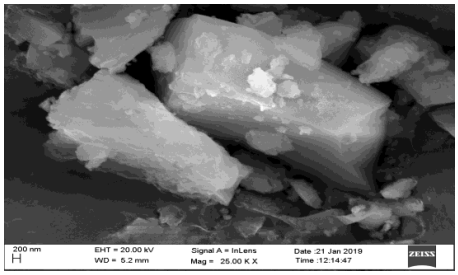

(B)

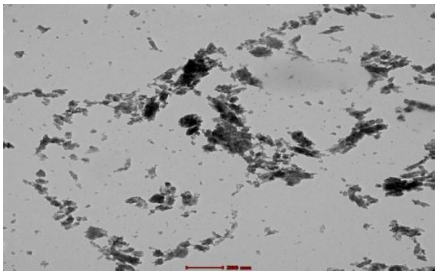

(C)

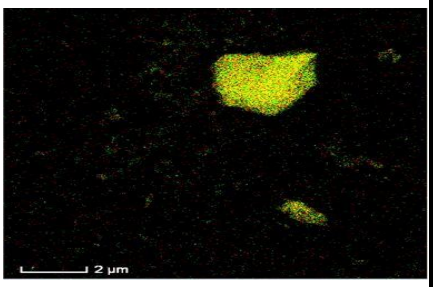

(D)

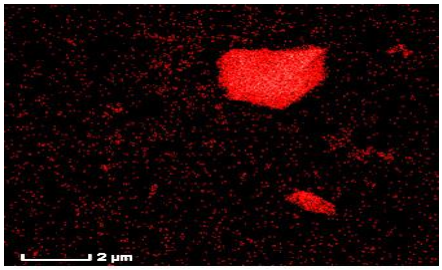

(E)

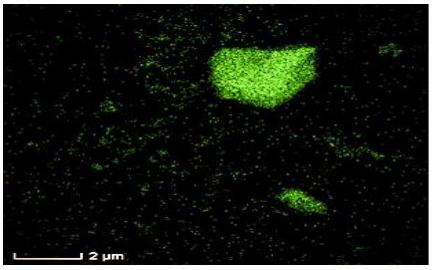

(F)

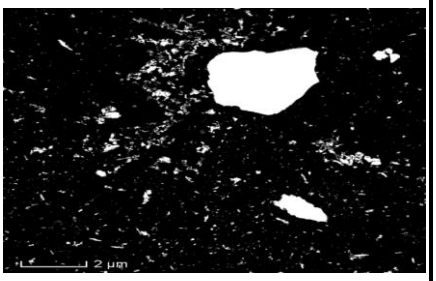

(G)

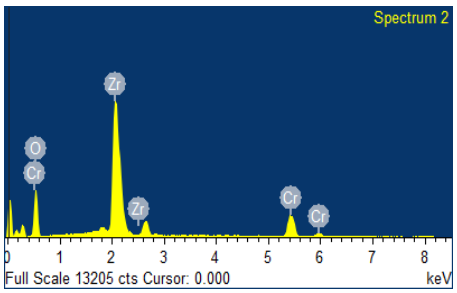

(H)

Elements	Weight%	Atomic%
Cr K	12.51	9.29
Zr L	60.50	25.60
O	26.99	65.12
Total	100.00	

(I)

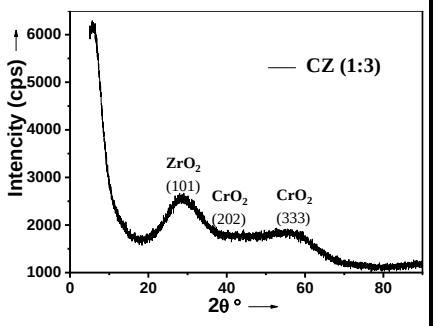

Figure 1: (A) Scanning Electron microscopic images of CZ, (B) Transmittance electron Microscopic images of CZ, (C) Elemental mapping of CZ, (D) Elemental mapping of Zirconium in CZ, (E) Elemental Mapping of Chromium in CZ and (F) Elemental mapping of Oxygen in CZ, (G) SEM-EDS spectra and (H) Atomic percentage, (I) Powder X-Ray Diffraction pattern of CZ.

(a)

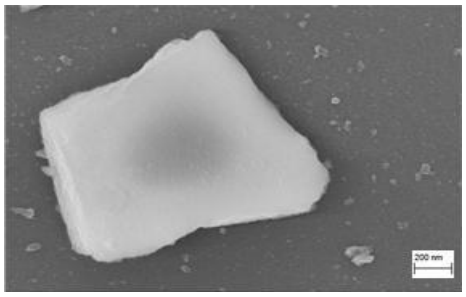

(b)

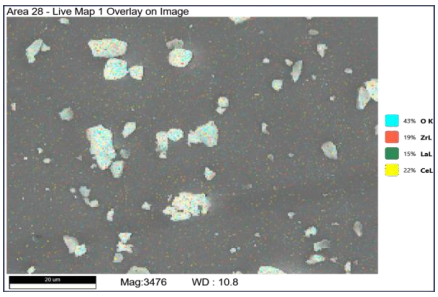

(c)

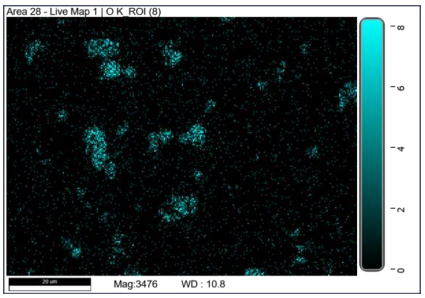

(d)

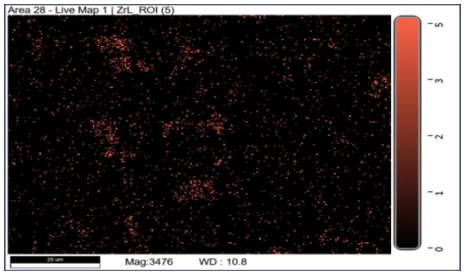

(e)

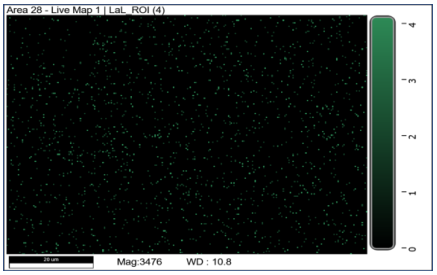

(f)

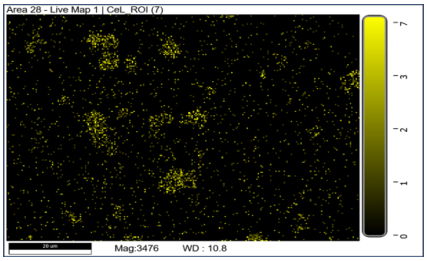

(g)

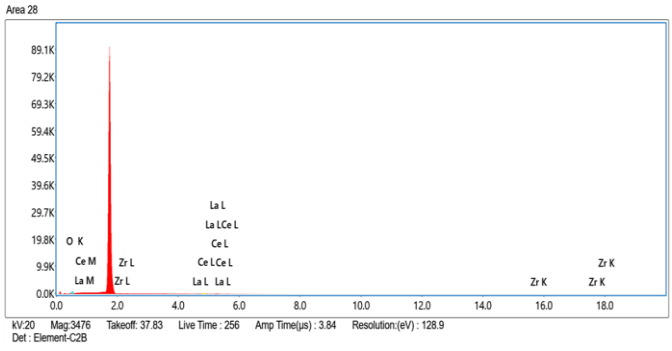

(h)

Element	Weight % Net Int.	Atomic %
O K	38.00	82.97
Zr L	11.67	4.47
La L	6.02	1.51
Ce L	44.31	11.05

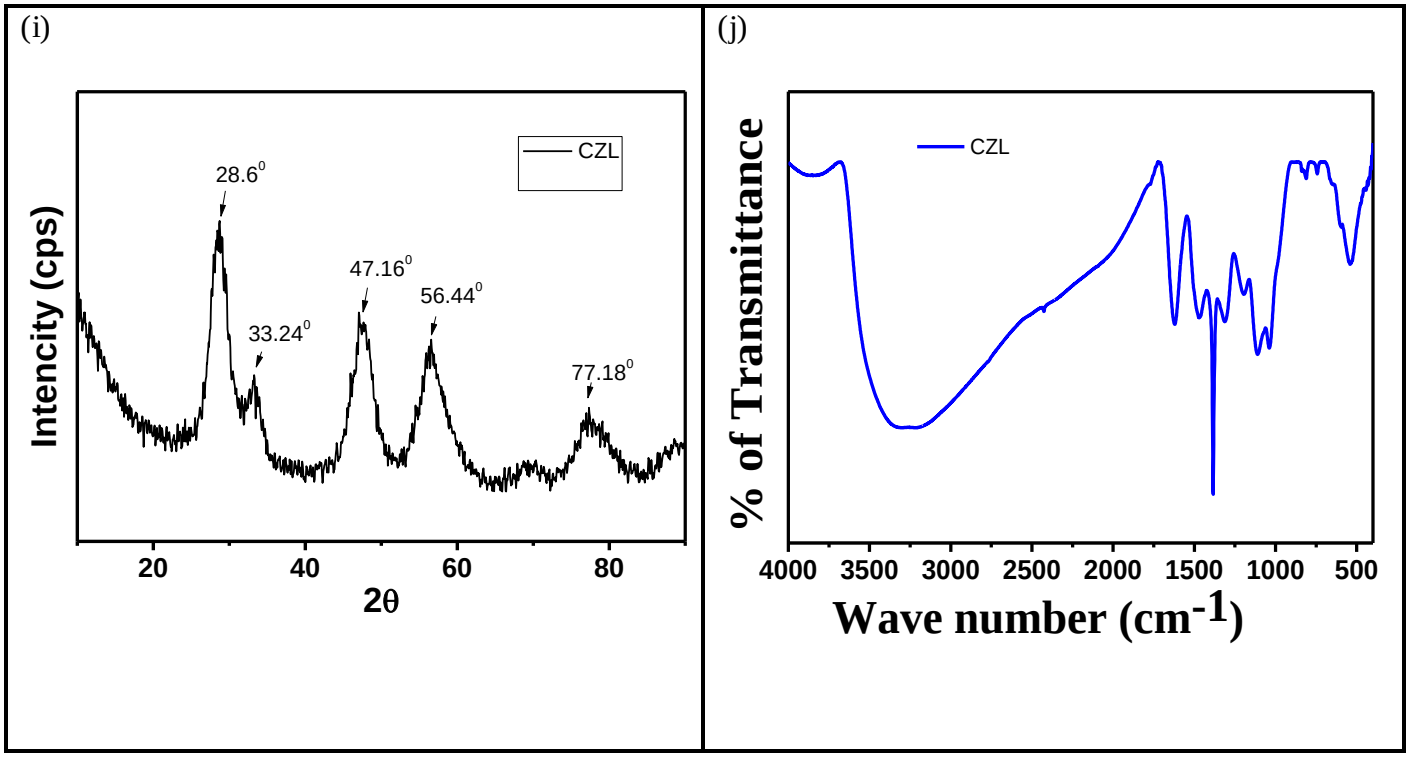

Figure 2: (a) Scanning Electron microscopic images of CZL, (b) Elemental mapping of CZL, (c) Elemental mapping of Oxygen in CZL, (d) Elemental Mapping of Zirconium in CZL and (e) Elemental mapping of Lanthanum in CZL (f) Elemental mapping of Cerium in CZL, (g) SEM-EDS spectra and (h) Atomic percentage, (i) Powder X-Ray Diffraction pattern of CZL and (j) FT-IR spectrum of CZL.

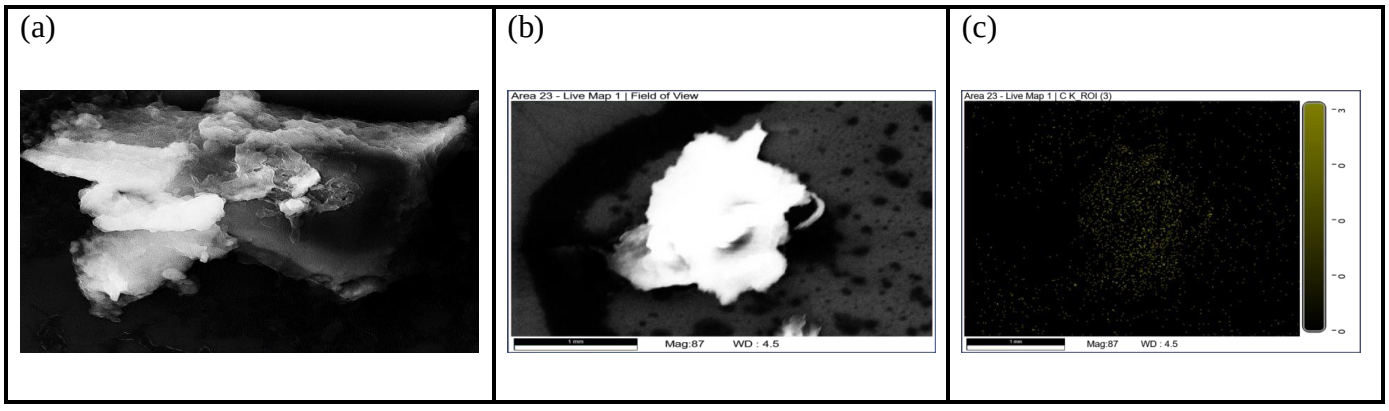

(d)

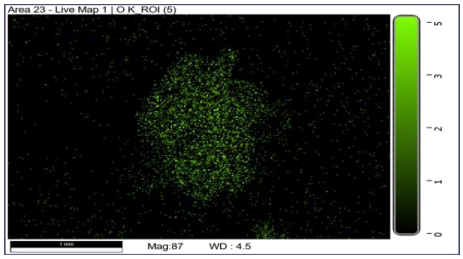

(e)

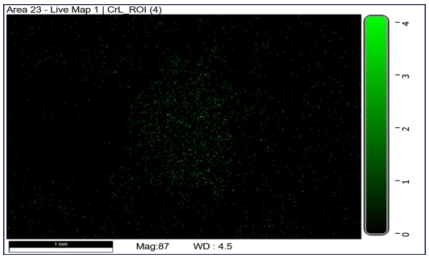

(f)

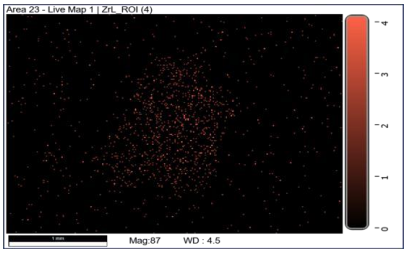

(g)

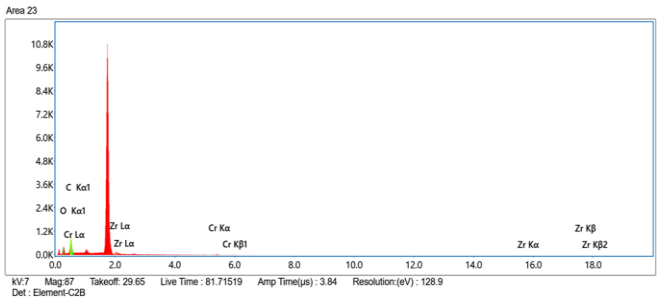

(h)

Element	Weight %	Atomic %
C K	25.05	41.00
O K	40.91	50.27
Cr L	8.55	3.23
Zr L	25.49	5.49

(i)

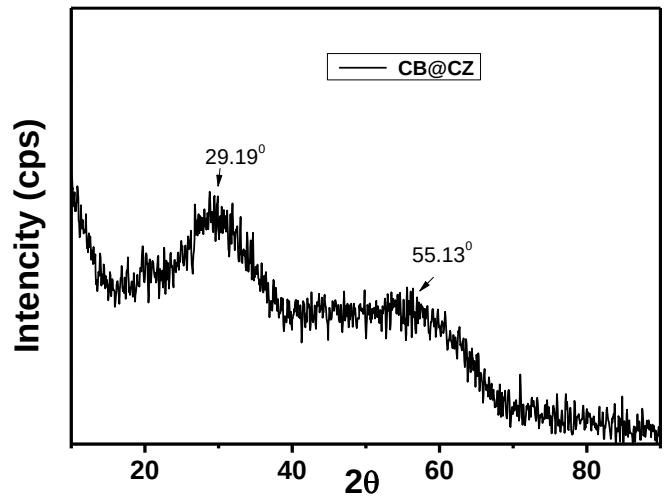

(j)

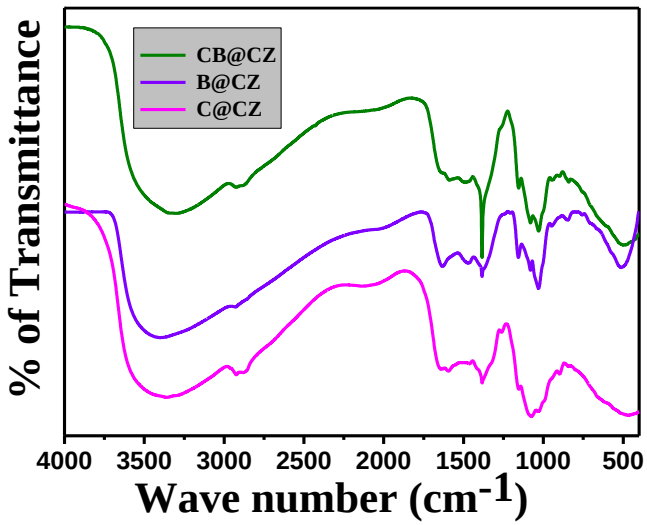

Figure 3: (a) Scanning Electron microscopic images of CB@CZ, (b) Elemental mapping of CB@CZ, (c) Elemental mapping of carbon in CB@CZ, (d) Elemental Mapping of Oxygen (e) Elemental mapping of Chromium (f) Elemental mapping of Zirconium, (g) SEM-EDS spectra and (h) Atomic

percentage, (i) Powder X-Ray Diffraction pattern of CB@CZ,(j) Comparison of FT-IR spectrum of C@CZ, B@CZ and CB@CZ.

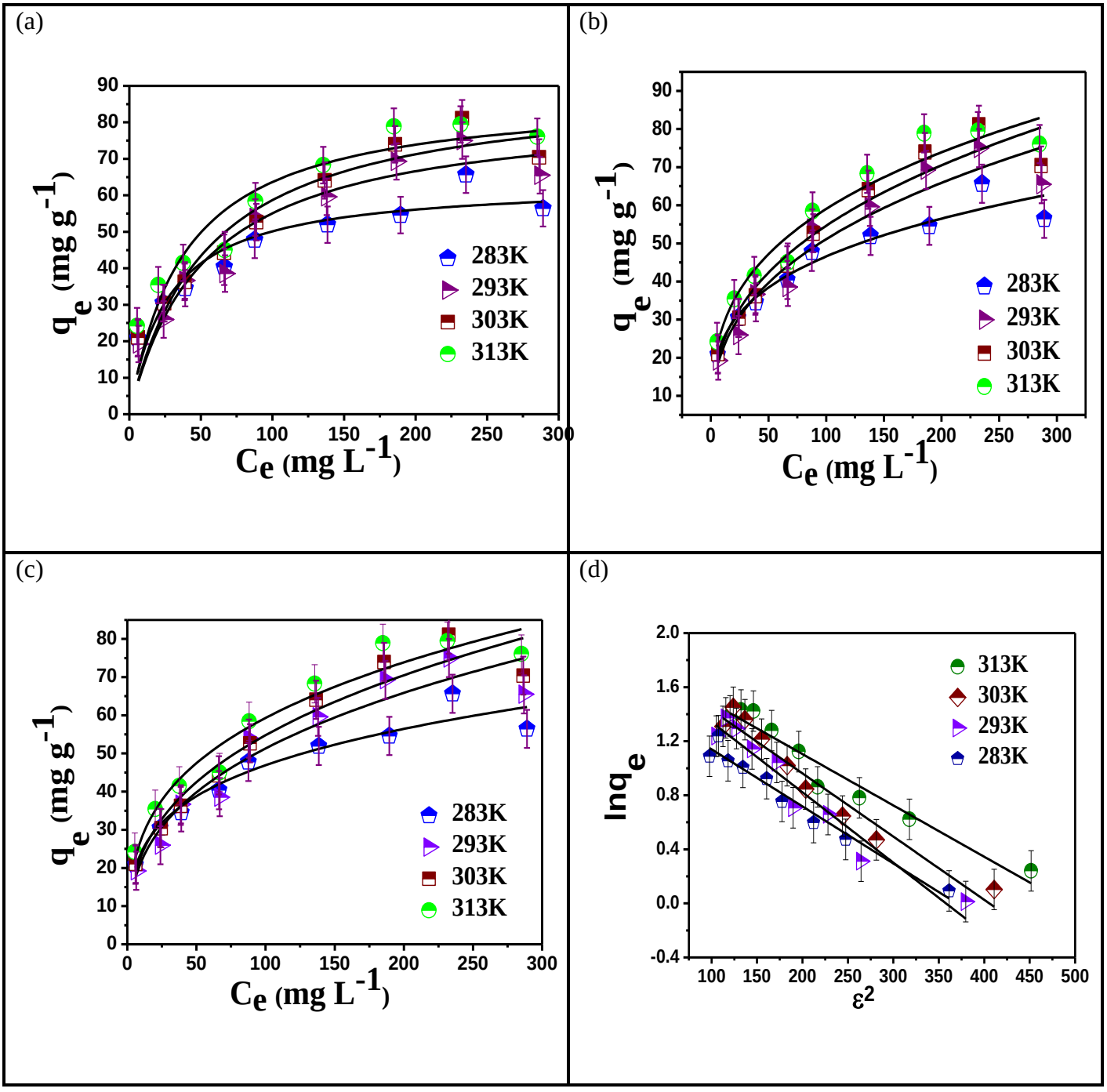

Figure 4: Adsorption Isotherm plot of CZ (a) Langmuir, (b) Freundlich (c) Redlich Peterson (d) DR isotherm.

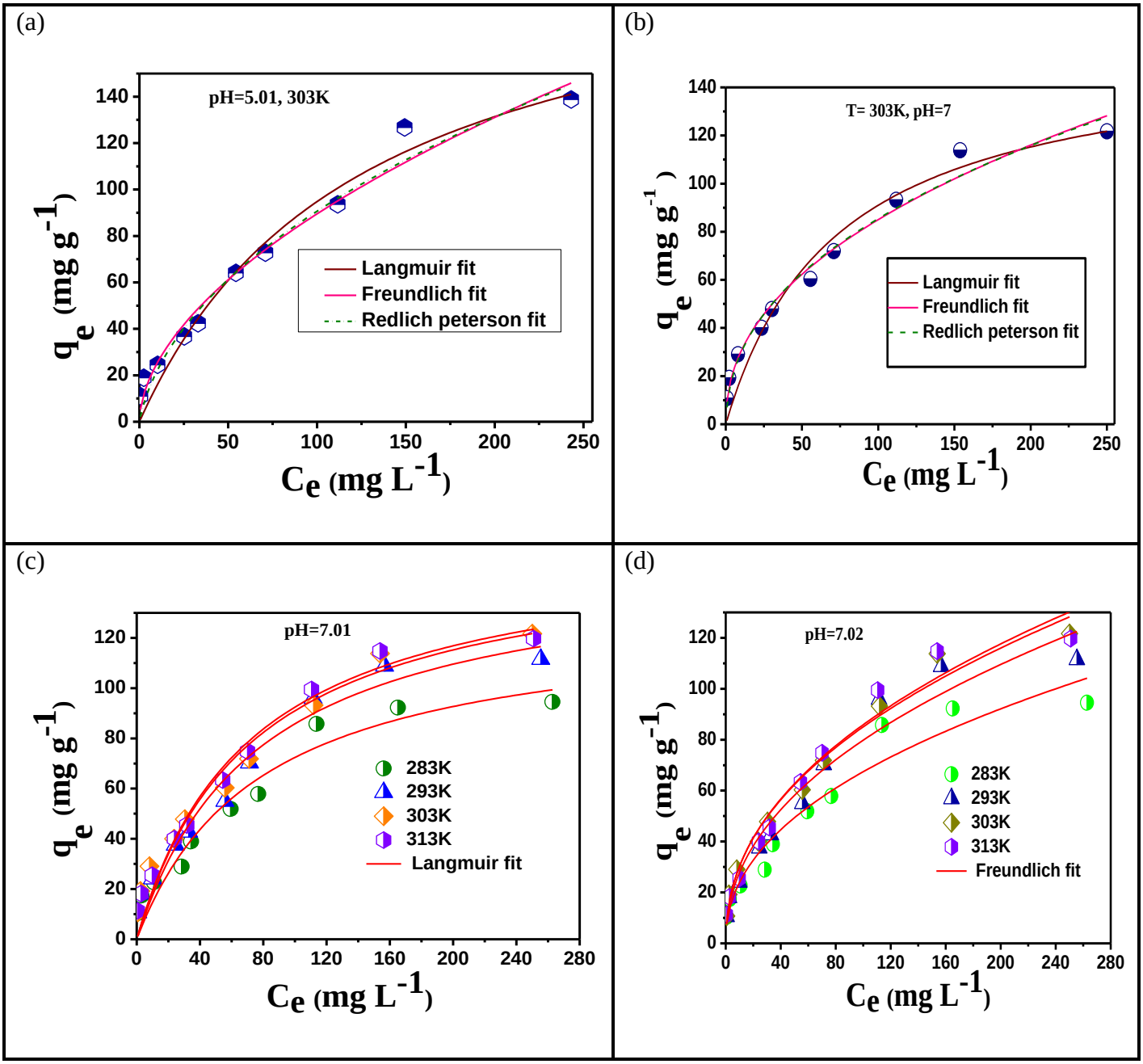

Figure 5: Isotherm plot for fluoride adsorption of CZL (a) at pH 5.01 and 303K, (b)) at pH 7.02 and 303K (c) at four different temperature, at pH 7.02 and model fit by Langmuir, (d)) at four different temperature, at pH 7.02 and model fit by Freundlich.

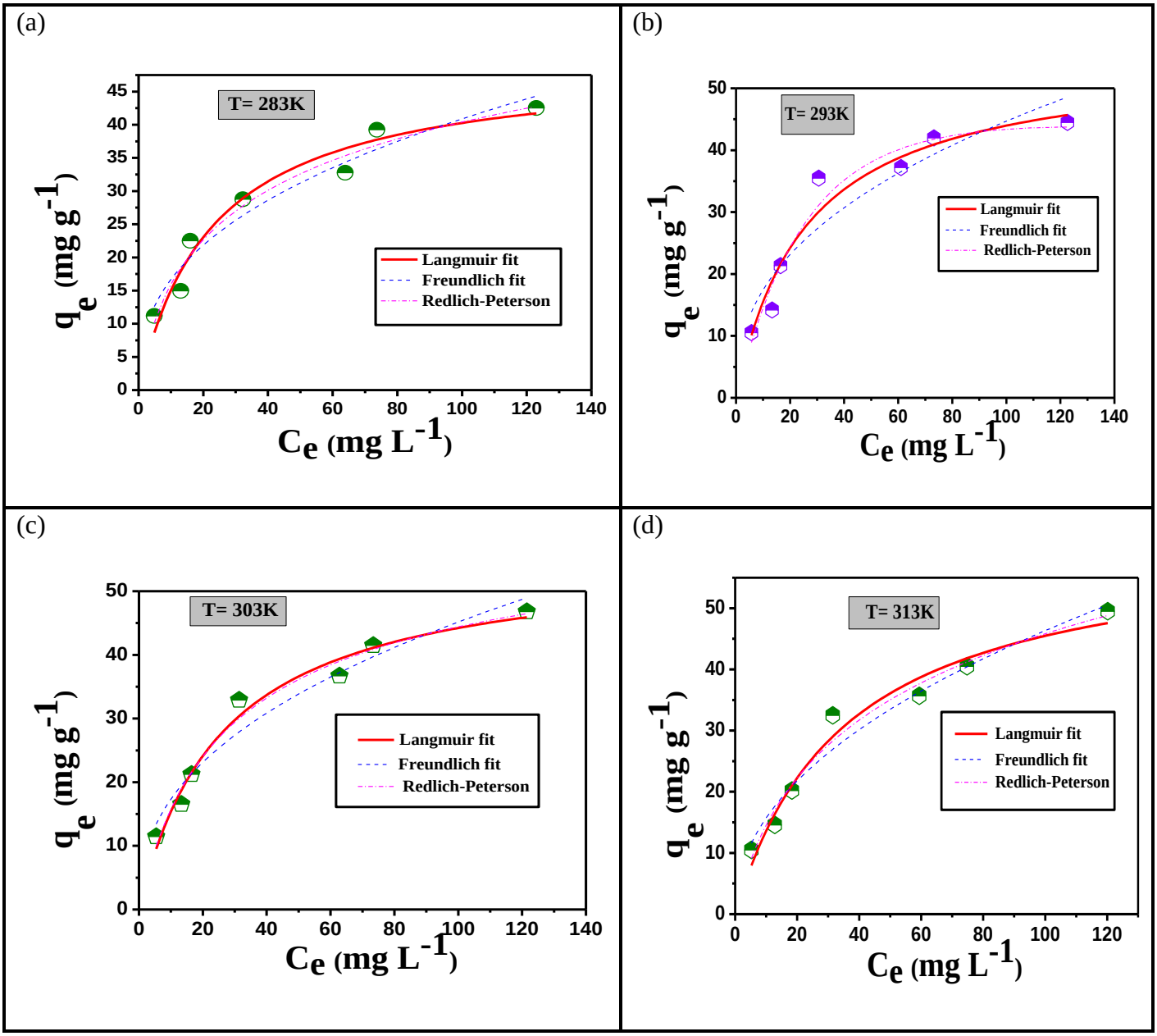

Figure 6: Isotherm plot for Cu(II) adsorption at pH 5.01 and Freundlich (dotted line) and Langmuir model equation fitting with four different temperature of CZL (a) 283K, (b) 293K, (c) 303K, (d) 313K.

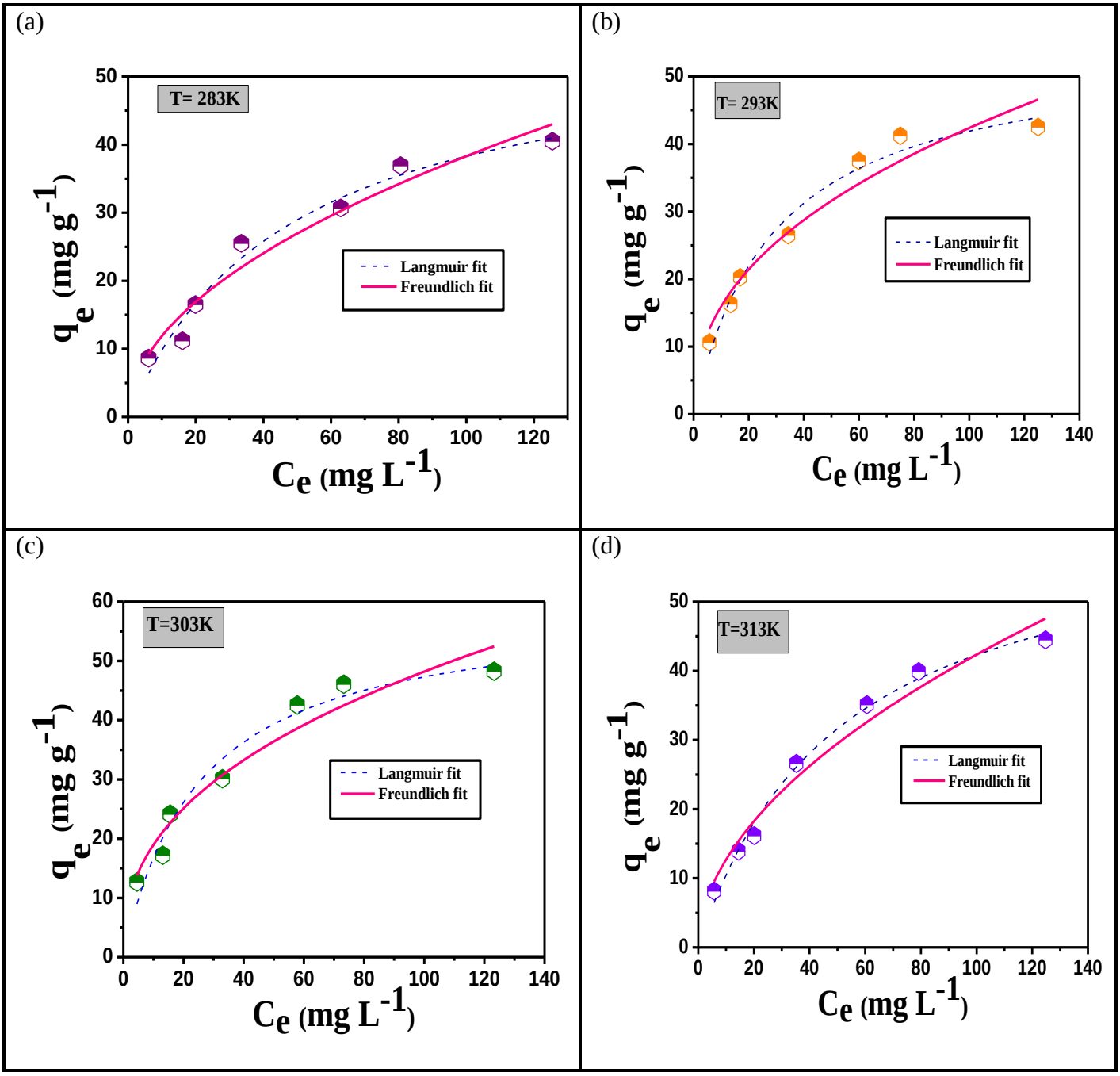

Figure 7: Isotherm plot for Cu(II) adsorption at pH 5.01 and Freundlich (dotted line) and Langmuir model equation fitting with four different temperature of CB@CZ (a) 283K, (b) 293K, (c) 303K, (d) 313K.

Lists of Publications

1) **Sarat Kanrar**, Abir Ghosh, Ayan Ghosh, Arpan Mondal, Mriganka sadhukhan, Uday Chand Ghosh1, Sasikumar Palani1, One-pot synthesis of Cr(III)-incorporated Zr(IV) oxide for fluoride remediation: a lab to field performance evaluation study. Environmental science and pollution research international 27 (2020) 15029-15044. **https://doi.org/10.1007/s11356-020-07980-5.**

2) **Sarat Kanrar**, Sushanta Debnath, Pradip De, Kamya Parashar , Kriveshini Pillay, Palani Sasikumar, Uday Chand Ghosh, Preparation, characterization and evaluation of fluoride adsorption efficiency from water of iron-aluminium oxide-graphene oxide composite material. Chemical Engineering Journal 306 (2016) 269–279. **http://dx.doi.org/10.1016/j.cej.2016.07.037.**

3) Abir Ghosh, **Sarat Kanrar**, Debabrata Nandi, Palani Sasikumar, Krishna Biswas and Uday Chand Ghosh, Redox-Assisted Arsenic(III) Adsorption for Removal from Aqueous Solution by Cerium(IV)-Incorporated Zirconium Oxide Nanocomposites. Journal of Chemical & Engineering Data 65 (2020) 885-895. **https://dx.doi.org/10.1021/acs.jced.9b01075.**

4) Indranil Saha, **Sarat Kanrar**, Kaushik Gupta, Bibhutibhushan Show, Debabrata Nandi, Krishna Biswas, Biswaranjan Manna, Debasish Chatterjee, Uday Chand Ghosh, Tuned synthesis and characterization insight into β-cyclodextrin amended hydrous iron zirconium hybrid oxide: a promising scavenger of fluoride in aqueous solution. RSC Adv. 6 (2016) 93842-93854. **https://dx.doi.org/10.1039/C6RA16567B.**

National & International Seminar, Conference & Presentation

- Research paper presented for the poster presentation on **8-9th January, 2020** in Two-day **International seminar** on **—** Innovation, Expansion, Impacts and Challenges in Chemical and Biological Sciences," organized by Department of Chemistry, Surendranath College.

- Research paper presented for the oral presentation on December **23-24, 2019** in **4th Regional Science and Technology Congress (Southern Regeion),** organized by Department of science & technology and bio-technology, Govt.of West Bengal & Maulana Abul Kalam Azad University of Technology, West Bengal at Haringhata, Nadia.

- Research paper presented for the poster presentation on **August 2 & 3th, 2019** in **International Symposium** on Recent Advance in Chemistry and Material Sciences and the celebration of the International year of the Period Table in commemoration of the 158th Birth Anniversary of Acharya Prafulla Chandra Ray organized by The Indian Chemical Society and Chemical Science Division, Saha Institute of Nuclear Physics, Kolkata.

- Research paper presented for the Poster presentation entitled Preparation of Graphene Oxide incorporated Fe(III)-Al(III) mixed oxide and fluoride adsorption behaviours ” held on **19-20th January, 2018** at **International Conference** on Current trends in materials Science and Engineering (CTMSE 2018) held in S.N Bose national Centre for basic Science.

Forwarded

Signature of the Candidate

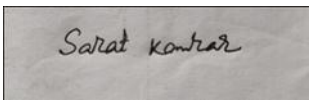

(SARAT KANRAR)

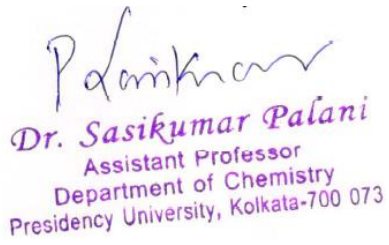

(Dr. SASIKUMAR PALANI)

Supervisor

Assistant Professor of Chemistry

Presidency University, Kolkata

SL. NO. Science/S-61/19.

Presidency University

Hindoo College (1817-1855), Presidency College (1855-2010)
86/1 College Street, Kolkata 700 073

REGISTRATION CERTIFICATE

This is to certify that Mr. Sarat Kanrar, s/o Bijoy Kanrar, has been granted registration for the Ph.D. Programme in the **Department of Chemistry** of Presidency University, Kolkata in terms of the Regulations (No. 4) for the Degree of Doctor of Philosophy (Ph.D.).

Registration Number: **R-17RS205110096**

Date of Registration: **10th July, 2018**

Title of the thesis: **"Synthesis, Characterisation of Mixed Metal Oxide Based Inorganic Materials and It's Application Towards the Removal of Fluoride and Heavy Metals From Contaminated Water"**

This registration shall remain valid for five years with effect from the date of registration as indicated above.

Registrar

Date: 29th January 2019

PRESIDENCY UNIVERSITY
KOLKATA

Presidency University

Hindoo College (1817-1855), Presidency College (1855-2010)
86/1, College Street, Kolkata 700073, West Bengal, India
website: www.presiuniv.ac.in

PhD.CW/CHEMISTRY2018009

Grade Card –cum- Certificate

Certified that SARAT KANRAR bearing Enrolment Number PU/PHD/CHEM/2017/009 of the Department of CHEMISTRY has successfully qualified the Ph.D. Coursework Examination in CHEMISTRY held in Odd Semester 2017- 2018, with the following grades.

Name: SARAT KANRAR

Enrolment Number: PU/PHD/CHEM/2017/009

Paper	Credit	Grade obtained
Research Methodology	4	A+
Physical Chemistry of Polymer	4	A
Magneto-chemistry	4	A++
Review of Research Work	4	A+

Total Credits: 16

SGPA : 9.00

CGPA: 9.00

Date of Publication: 19TH February, 2018

Controller of Examinations

4th REGIONAL SCIENCE AND TECHNOLOGY CONGRESS
(SOUTHERN REGION), 2019

Jointly Organised By

DEPARTMENT OF SCIENCE & TECHNOLOGY AND BIO-TECHNOLOGY, GOVT. OF WEST BENGAL

&

MAULANA ABUL KALAM AZAD UNIVERSITY OF TECHNOLOGY, WEST BENGAL

This is to certify that Prof./Dr./Mr./Ms. ..... Sarat Kantar .....

of ..... Presidency university ..... is the presenting Author / Co-author / Corresponding Author in Oral / Poster / Exhibition session of the 4th Regional Science and Technology Congress (Southern Region) 2019, jointly organised by Department of Science and Technology and Bio-Technology, Government of West Bengal & Maulana Abul Kalam Azad University of Technology, West Bengal during December 23-24, 2019 at Haringhata, Nadia-741249.

Dr. Somdatta Chakravortty
Organising Secretary
4th Regional Science and Technology Congress (Southern Region), 2019
Maulana Abul Kalam Azad University of Technology, West Bengal

Dr. Suchandra Choudhury
Organising secretary
4th Regional Science and Technology Congress (Southern Region), 2019
Department of Science & Technology and Bio-Technology, Govt. of West Bengal

Bicentenary Celebration of Presidency University

POSTER PRESENTATION

as a part of **Two Day Symposium**

Organized by

Department of Chemistry, Presidency University

During 4th & 5th January, 2018

This is to certify that

Mr./Ms. Sarat Kanrar of Presidency University

participated in the **Poster Presentation** of the **Two Day Symposium**, organized by Department of Chemistry, Presidency University held on 5th of January, 2018 at Presidency University and he secured fist position in the Poster Competition.

We wish him/her a bright future ahead.

Prof. Bijan Das
Chairperson
Head, Dept. of Chemistry

Dr. Dhruba Prosad Chatterjee
Convener

Dr. Koena Ghosh, Dr. Arnab Halder
Joint Coordinators

2019
NCSCA
Conference for Collaboration

11th NATIONAL CONFERENCE ON
SOLID STATE CHEMISTRY AND ALLIED AREAS

Theme of Conference: Functional Materials & Life Sciences

Certificate

This is to certify that Prof. / Dr. / Mr. / Mrs. / Miss.

Sarat Kanrar

Dept. of Chem, Presidency University, Kolkata

has attended / presented Paper **Oral/Poster** in **SERB-DST, BRNS, CSIR,** and **MoES** Sponsored ***11th NATIONAL CONFERENCE ON SOLID STATE CHEMISTRY AND ALLIED AREAS (NCSCA - 2019)*** held at Nagpur, INDIA, during **20th and 21st December 2019.**

Organized By

SETH KESARIMAL PORWAL COLLEGE OF ARTS, SCIENCE & COMMERCE, KAMPTEE

In Association With

INDIAN ASSOCIATION OF SOLID STATE CHEMISTS AND ALLIED SCIENTISTS (ISCAS), JAMMU

Dr. M B Bagade	Dr. M Swaminathan	Dr. R G Chaudhary	Dr. P R Dhongle	Prof. N P Meshram
Chairman	President ISCAS	Convener	Organizing Secretary	Coordinator

Sponsored By

Science and Engineering Research Board (SERB)

Board Of Research In Nuclear Sciences (BRNS)

Council of Scientific & Industrial Research (CSIR)

Ministry of Earth Sciences (MoES)

International Symposium on
Recent Advances in Chemistry and Material Sciences (2019)
and
The Celebration of the International Year of the Periodic Table

In Commemoration of the 158th Birth Anniversary of Acharya Prafulla Chandra R[illegible]

This is to certify that Professor/Dr./Mr./Ms. Sarat Kanrar
of Presidency University has been participated/presented/delivered (Endowment Lecture/Invited Lecture/Oral/Poster) in the International Symposium on "Recent Advances in Chemistry and Material Sciences (2019)" organized by the Indian Chemical Society and Chemical Sciences Division, Saha Institute of Nuclear Physics, Kolkata on August 02 & 03, 2019.

3rd August, 2019
Kolkata

Professor Chittaranjan Sinha
Honorary Secretary
Indian Chemical Society

Professor Dulal C. Mukherjee
President
Indian Chemical Society

Professor Susanta Lahiri
Head, Chemical Sciences Division
Saha Institute of Nuclear Physics

IEM
INSTITUTE OF ENGINEERING & MANAGEMENT
श्रद्धावान लभते ज्ञानम्
Good Education, Good Jobs

Celebrating 125th Birth Anniversary

CENTRE FOR BASIC SCIENCES
S. N. BOSE NATIONAL
1894 - 1974
विज्ञानेन परिप्रवर्तते लोकः

International Conference on
Current Trends in Materials Science and Engineering (CTMSE 2018)

Organised by

INSTITUTE OF ENGINEERING & MANAGEMENT, KOLKATA
AND
S. N. BOSE NATIONAL CENTRE FOR BASIC SCIENCES, KOLKATA

Certificate of Appreciation

This is to certify that Prof./Dr./Mr./Mrs/Ms. Sarat Kanrar
of Presidency University *has presented a Poster entitled*

"Preparation of Graphene Oxide incorporated Fe(III) - Al(III) mixed oxide & fluoride adsorption behaviour"

in CTMSE 2018 held on 19th - 20th January, 2018 at S.N. Bose National Centre for Basic Sciences.

Arun Kumar Bar
Arun Kumar Bar
Chairman,
Institute of Engineering & Management

Anjan Barman
Anjan Barman
Convenor,
S. N. Bose National Centre for Basic Sciencesz

Saswati Barman
Saswati Barman
Convenor,
Institute of Engineering & Management

Journal of chemical & engineering data

pubs.acs.org/jced Article

Redox-Assisted Arsenic(III) Adsorption for Removal from Aqueous Solution by Cerium(IV)-Incorporated Zirconium Oxide Nanocomposites

Abir Ghosh, Sarat Kanrar, Debabrata Nandi, Palani Sasikumar, Krishna Biswas,* and Uday Chand Ghosh*

Cite This: https://dx.doi.org/10.1021/acs.jced.9b01075 Read Online

ACCESS | Metrics & More | Article Recommendations | Supporting Information

ABSTRACT: Ceria-incorporated zirconia nanocomposites (CIZNCs) are prepared and characterized by some latest analytical tools. The efficiency of this material is evaluated toward arsenic(III) immobilization for removal via adsorption from its aqueous phases. The physicochemical aspects of this immobilization reaction have been reported at optimized pH 5.0. The kinetics of this reaction is of pseudo-second order type. The equilibrium data fit very well with the Langmuir isotherm with a monolayer adsorption capacity of 17.07 mg·g^{-1} (226 mmol·kg^{-1}) at 303 K. Analysis of reaction kinetics parameters shows that the fraction of molecules bearing the threshold energy of reaction (Δ_N/N_{av}) is 0.99 at our working conditions. Thermodynamic analysis of equilibrium data reveals the exothermic and spontaneous nature of arsenic(III) adsorption over CIZNCs. X-ray photoelectron spectroscopy and cyclic voltammetric examinations have confirmed the oxidation of arsenic(III) to arsenic(V) over the CIZNC surface.

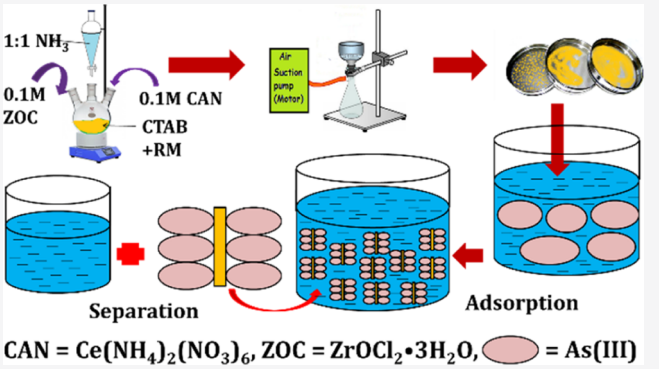

INTRODUCTION

Natural occurrences of arsenic especially arsenic(III) in groundwater much exceeding the tolerance limit have been identified as a worldwide problem.[1] Although arsenic poisoning through drinking water has been emanating since long back, the first cases of skin cancer were observed among the population in Poland (1898) owing to consumption of excess arsenic-contaminated water. Since then, it has been conclusively established that unabated ingestion of arsenic via drinking water causes a variety of carcinogenic effects of skin, liver, kidney, and other organs which ultimately leads to death.[2−4] These incidents have led to the World Health Organization (WHO) and other national agencies to fix the permissible level to 0.01 mg·As·L^{-1} of drinking water.[5] Groundwater, being a main source of drinking water, has been contaminated with excess arsenic (>0.01 mg·L^{-1}) because of anthropogenic reasons. A majority of rural and semiurbanized population of this globe have been consuming such water for drinking and other household needs. The problem associated with arsenic contamination is severe in Bangladesh and major parts of West Bengal (India).[6,7] In West Bengal, more than 6 million people from 12 districts covering 111 blocks are the worst affected because of consuming drinking water with arsenic concentration >0.05 mg·L^{-1}.[8−10] Though arsenic mainly exists in groundwater in +III and +V states, the former species is more toxic and mobile than the latter one,[11,12] and the inorganic arsenic is ∼100 times more toxic than the organic form[13] because soft arsenic(III) preferably binds more readily than hard arsenic(V) with the thiol (−SH) group of cystein. The pH-dependent species of arsenic in oxic water are $H_2AsO_4^-$ and $HAsO_4^{2-}$, while those in anoxic water are H_3AsO_3 and $H_2AsO_3^-$.[14] Among the various treatment processes/technologies developed and refined over the years for arsenic remediation, adsorption has emerged particularly as an attractive process for arsenic eradication chiefly because of simplicity. The materials used as adsorbents are the various forms of iron oxide and hydroxide,[15−18] red mud,[19] activated alumina,[20−22] iron oxide-coated polymeric materials,[23] iron oxide-coated sand,[24] Fe(III)−Si binary oxide,[25] and iron oxide-impregnated activated alumina.[26] In our laboratory, we have developed arsenic removal methods using crystalline hydrous ferric oxide,[27] crystalline hydrous titanium oxide,[28]

Received: November 13, 2019
Accepted: January 16, 2020

Downloaded via UNIV OF GOTHENBURG on February 1, 2020 at 01:52:18 (UTC).
See https://pubs.acs.org/sharingguidelines for options on how to legitimately share published articles.

© XXXX American Chemical Society

Environmental Science and Pollution Research
https://doi.org/10.1007/s11356-020-07980-5

RESEARCH ARTICLE

One-pot synthesis of Cr(III)-incorporated Zr(IV) oxide for fluoride remediation: a lab to field performance evaluation study

Sarat Kanrar[1] · Abir Ghosh[1] · Ayan Ghosh[1] · Arpan Mondal[2] · Mriganka Sadhukhan[3] · Uday Chand Ghosh[1] · Palani Sasikumar[1]

Received: 13 November 2019 / Accepted: 3 February 2020
© Springer-Verlag GmbH Germany, part of Springer Nature 2020

Abstract

A low-cost Cr(III)-incorporated Zr(IV) bimetallic oxide (CZ) was synthesized by simple chemical precipitation method for removal of fluoride from contaminated water. The physicochemical properties of CZ before and after fluoride removal were established with several instrumental techniques such as TEM with elemental mapping, SEM with EDX, XRD, IR, XPS, zeta potential measurement, etc. Batch adsorption technique were carried out to understand the factors affecting fluoride adsorption, such as effects of initial pH, adsorbent dose, co-occurring ions, contact time, and temperature. The maximum adsorption capacity observed at pH between 5 and 7. The fluoride adsorption processes on CZ obeyed the pseudo-second-order rate equations and both Freundlich and DR isotherm models. The maximum adsorption capacity of 90.67 mg g^{-1} was obtained. The thermodynamic parameters ΔH^0 (positive), ΔS^0 (positive), and ΔG^0 (negative) indicating the fluoride sorption system was endothermic, spontaneous, and feasible. The CZ also successfully used as fluoride adsorbent for real field contaminated water collected from the Machatora district, Bankura, West Bengal, India.

Keywords Fluoride · Adsorption · Mixed oxide · Co-occurring ions · Kinetics · Thermodynamics

Highlights
- Cr(III)-incorporated Zr(IV) oxide a pristine low-cost material for fluoride removal
- Maximum fluoride adsorption capacity obtained 90.67 mg g^{-1}
- Reaction kinetics experiment performed in presence of co-occurring ions
- Fluoride adsorption mechanism studied instrumentally
- Real contaminated ground water was collected and treated successfully

Responsible editor: Tito Roberto Cadaval Jr

Electronic supplementary material The online version of this article (https://doi.org/10.1007/s11356-020-07980-5) contains supplementary material, which is available to authorized users.

✉ Palani Sasikumar
sasikumar.chem@presiuniv.ac.in

[1] Department of Chemistry, Presidency University, 86/1 College Street, Kolkata, West Bengal 700073, India

[2] Department of Chemistry, Indian Institute of Science Education and Research (IISER), Bhopal By-pass Road, Bhauri 462066, Madhya Pradesh, India

[3] School of Chemical Sciences, National Institute of Science Education and Research (NISER), Bhubaneswar, Odisha 751 005, India

Introduction

Fluoride is a common contaminant found in alarming level in soil and drinking water around the world (Jagtap et al. 2012; Rivera-Utrilla et al. 2019; Barathi et al. 2019). High concentration of fluoride contamination originates due to leaching of fluoride from minerals and untreated discharge of hazardous wastes from industries (Tekle-Haimanot et al. 2006; Podgorski et al. 2018). Minimum consumption (< 1 mg L^{-1}) of fluoride in drinking water is beneficial for human dental health and therapeutic osteoporosis treatment (Kanduti et al. 2016; Slade et al. 2018). However, high-level (> 1.5 mg L^{-1}) intake and prolong exposure causes several detrimental effects including dental, skeletal fluorosis, neurotoxicity, lower IQ, osteosarcoma, infertility, brain damage, Alzheimer syndrome, and thyroid disorder (Green et al. 2019). Keeping the view of health adverse effects past few decades, several treatment technologies have been developed for the removal of excess fluoride from drinking water (Biswas et al. 2010; Rivera-Utrilla et al. 2019). However, adsorption technique is well popularized and promising one, due to low cost, simplicity of design, ease of operation, and high efficiency, especially for small community systems in rural areas (Bhatnagar et al.

Published online: 17 February 2020

Chemical Engineering Journal 306 (2016) 269–279

Contents lists available at ScienceDirect

Chemical Engineering Journal

journal homepage: www.elsevier.com/locate/cej

Preparation, characterization and evaluation of fluoride adsorption efficiency from water of iron-aluminium oxide-graphene oxide composite material

Sarat Kanrar [a], Sushanta Debnath [b], Pradip De [a], Kamya Parashar [c], Kriveshini Pillay [c], Palani Sasikumar [a], Uday Chand Ghosh [a,*]

[a] Department of Chemistry, Presidency University, 86/1 College Street, Kolkata 700073, India
[b] Crystallography and Molecular Biology Division, Saha Institute of Nuclear Physics, Kolkata 700064, India
[c] Department of Applied Chemistry, University of Johannesburg, Johannesburg, South Africa

HIGHLIGHTS

- Iron(III)-aluminium(III)-graphene oxide (HIAGO) composite for fluoride adsorption.
- HIAGO with 3 g graphene oxide showed highest fluoride adsorption efficiency.
- Langmuir isotherm and pseudo-second order kinetics described the data best.
- Found 25% higher monolayer capacity of HIAGO than native mixed oxide.
- Estimated process parameters are highly prospective.

GRAPHICAL ABSTRACT

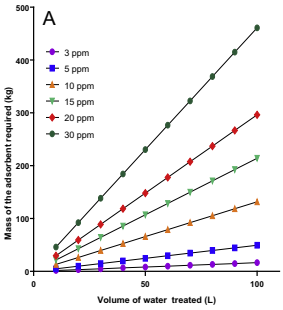

ARTICLE INFO

Article history:
Received 13 April 2016
Received in revised form 1 July 2016
Accepted 9 July 2016
Available online 17 July 2016

Keywords:
Adsorption
Composite
Co-precipitation
Fluoride
Graphene oxide
Iron-aluminium oxide

ABSTRACT

Graphene oxide (GO)-incorporated iron-aluminium mixed oxide (HIAGO) composite, a nobel material was prepared and characterized by FTIR, XRD, TGA/DTA, SEM, TEM, and Raman spectroscopy, which had been employed for adsorption of the fluoride from aqueous solutions. When this material was examined for fluoride scavenging ability from water, it had been established that the as-prepared HIAGO obtained by incorporating 3.0 g GO per 0.2 fraction of one gram formula amount of the mixed oxide matrix showed highest fluoride adsorption capacity (q_e, mg g^{-1}) at pH ~ 7.0 and ambient temperature. The material showed an increase of q_e with pH up to ~5.5, and then reduced. Kinetically, fluoride adsorption took place obeying the pseudo-second order model. The Langmuir adsorption isotherm described the equilibrium data best with monolayer adsorption capacities 22.13, 22.90 and 27.75 mg g^{-1} at 288, 308 and 318 K, respectively, indicating endothermic nature of adsorption process, which was also confirmed from the thermodynamic analysis of equilibrium data. Fluoride adsorption efficiency of HIAGO had been predicted by modelling a single stage batch adsorber design parameters.

© 2016 Elsevier B.V. All rights reserved.

1. Introduction

Increasing industrialization era and growth of human civilization is compromising the sanctity of the nature and the environment. Vast industrialization and unplanned harvesting of ground water is becoming responsible for the contamination of the land

* Corresponding author.
E-mail address: ucghosh@yahoo.co.in (U.C. Ghosh).

http://dx.doi.org/10.1016/j.cej.2016.07.037
1385-8947/© 2016 Elsevier B.V. All rights reserved.

Published on 16 September 2016. Downloaded by National Institute of Science Education & Research on 23/07/2017 15:44:14.

RSC Advances

PAPER

View Article Online
View Journal | View Issue

Cite this: *RSC Adv.*, 2016, **6**, 93842

Tuned synthesis and characterizational insight into β-cyclodextrin amended hydrous iron-zirconium hybrid oxide: a promising scavenger of fluoride in aqueous solution†

Indranil Saha,[ab] Sarat Kanrar,[a] Kaushik Gupta,[a] Bibhutibhushan Show,[c] Debabrata Nandi,[d] Krishna Biswas,[e] Biswaranjan Manna,[a] Debashis Chatterjee[f] and Uday Chand Ghosh*[a]

The consumption of water contaminated with fluoride (>1.5 mg L^{-1}) causes serious problems to public health and ultimately leads to skeletal fluorosis. Thus, the development of more efficient fluoride scavenging materials for designing water filters is an immediate task for researchers. β-Cyclodextrin (β-CD) amended hydrous iron–zirconium hybrid oxide (CHIZO), which is a new type of surface modified highly selective composite in organic–inorganic frameworks, is synthesized and characterized using various state of the art analytical tools, and its efficacy on fluoride removal from an aqueous solution is explored. The agglomerated micro structured composite material has no significant fingerprint such as surface appearance in TEM images and is inclined to possess very poor crystallinity. The BET analysis of CHIZO reveals a surface area of 0.2070 m^2 g^{-1} and pore volume of 0.0476 cm^3 g^{-1}. The highly pH dependent fluoride adsorption by CHIZO decreases with an increase in pH, and pseudo-second order kinetics control the reaction. The Langmuir isotherm was recognized to be the best fit model to describe the adsorption equilibrium with a significantly higher monolayer adsorption capacity of fluoride (31.35 mg g^{-1}) than the host hydrous Fe–Zr oxide (8.21 mg g^{-1}) at pH ~7.0 and 303 K. The thermodynamically spontaneous nature of CHIZO is due to the exothermic nature of the reaction. In addition, phosphate and sulphate show an adverse effect on fluoride adsorption. β-CD forms inclusion complexes by taking up fluoride ions from water into its central cavity and the driving forces associated with the complex formation include the release of enthalpy-rich water molecules from its cavity, electrostatic interactions, hydrogen bonding and release of conformational strain. The poor regeneration of the spent adsorbent even in 1.0 M NaOH (below 20%) is probably a consequence of entrapping fluoride inside the cavity of β-CD with hydrogen bonding. It has been found that only 0.9 g of CHIZO is able to reduce the fluoride level to below 1.0 mg L^{-1} in one-litre of fluoride spiked (5.0 mg L^{-1}) natural water sample. The present study thus reveals that CHIZO could be an efficient adsorbent for fluoride because of its high adsorption capacity and economical viability.

Received 27th June 2016
Accepted 16th September 2016

DOI: 10.1039/c6ra16567b

www.rsc.org/advances

1 Introduction

Vast parts of the world have fallen prey to the two-pronged threats of arsenic and fluoride contamination, which are major contributors to water contamination in the globe. Along with arsenic contamination, fluoride is fast assuming menacing proportions in vitiating drinking water sources around the world since its discovery in the Nellore district of Andhra Pradesh (India) in 1937.[1] Spiked levels of fluoride in aquifers mostly result from its mobilization in natural conditions from fluoride bearing minerals. The recommended value of optimum fluoride levels in drinking water is fixed at 1.5 mg L^{-1} by the World Health Organization (WHO),[2] which is often not encountered in groundwater systems, thus leading to dental and bone fluorosis.[3] Groundwater constitutes 97% of global fresh water resources and forms a single point source for providing drinking water, and for most communities it may be the only economically viable option for this purpose. Thus, access to clean groundwater is of paramount importance, since it is critical in different spheres of human habitations. Excessive groundwater abstraction in relation to recharge has led to the

[a]Department of Chemistry, Presidency University, 86/1 College Street, Kolkata-700073, India. E-mail: ucghosh@yahoo.co.in; Fax: +91-33-2241 3893; Tel: +91-33-2241 3893
[b]Department of Chemistry, Sripat Singh College, Jiaganj, Murshidabad-742123, India
[c]Department of Chemistry, Jadavpur University, Kolkata-700032, India
[d]Department of Civil and Chemical Engineering, University of South Africa (UNISA), South Africa
[e]Department of Chemistry, Maharaja Manindra Chandra College, Kolkata-700003, India
[f]Department of Chemistry (Analytical), University of Kalyani, Nadia-741235, India

† Electronic supplementary information (ESI) available. See DOI: 10.1039/c6ra16567b

This journal is © The Royal Society of Chemistry 2016